



Biomimetic super-lyophobic and super-lyophilic materials applied for oil/water separation: A new strategy beyond nature

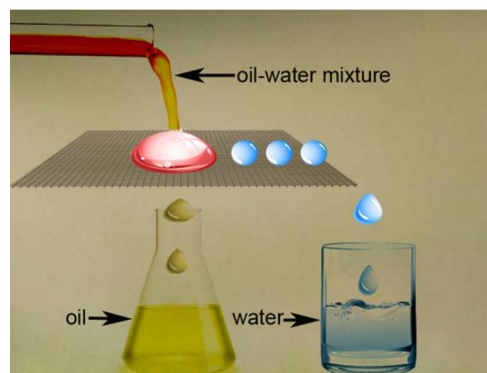
Journal:	<i>Chemical Society Reviews</i>
Manuscript ID:	CS-REV-07-2014-000220.R1
Article Type:	Review Article
Date Submitted by the Author:	17-Sep-2014
Complete List of Authors:	Wang, Ben; Hubei University, Liang, Weixin; Hubei University, zhiguang, Guo; Chinese Academy of Sciences, Lanzhou Insittute of Chemical Physics Liu, Weimin; Lanzhou Institute of Chemical Physics Lanzhou, State Key Laboratory of Solid Lubrication

Cite this: DOI: 10.1039/c0xx00000x

www.rsc.org/xxxxxx

ARTICLE TYPE

Abstract Graphic



5

Investigation in the field of oil/water separation materials with special wettabilities may accelerate the settlement of industrial oily wastewater and ocean oil spill accident.

Cite this: DOI: 10.1039/c0xx00000x

www.rsc.org/xxxxxx

ARTICLE TYPE

Biomimetic super-lyophobic and super-lyophilic materials applied for oil/water separation: A new strategy beyond nature

Ben Wang,^{†*a,b*} Weixin Liang,^{†*a,b*} Zhiguang Guo^{**a,b*} and Weimin Liu^{*b*}*Received (in XXX, XXX) XthXXXXXXXXXX 20XX, Accepted Xth XXXXXXXXXXXX 20XX*

DOI: 10.1039/b000000x

Oil spills and industrial organic pollutants have induced severe water pollutions and threatened every species in ecological system. To deal with the oily water, special wettability stimulated materials have been developed in the past decade to separate the oil-and-water mixtures. Basically, synergies between the surface chemical composition and surface topography are commonly known as the key factors to realize the opposite wettability to oils and water and dominate the selective wetting or absorbing of oils/water. In this review, we mainly focus on the developments of materials with either super-lyophobicity or super-lyophilicity in oil/water separation applications where they can be classified into four kinds as follow (in terms of the surface wettabilities of water and oils): superhydrophobic and superoleophilic materials, superhydrophilic and under water superoleophobic materials, superhydrophilic and superoleophobic materials, smart oil/water separation materials with switchable wettability. These materials have already been applied into the separation of oil-and-water mixture: from simple oil/water layered mixture to oil/water emulsions (including oil-in-water emulsions and water-in-oil emulsions), and from non-intelligent materials to intelligent materials. Meanwhile, they also exhibited high absorption capacity or separation efficiency and selectivity, simple and fast separation/absorption ability, excellent recyclability, economical efficiency and outstanding durability of harsh conditions. Then, related theories are proposed to understand the physical mechanisms of oil/water separation process. Finally, some challenges and promising breakthroughs in this field are also discussed. It is expected that special wettability stimulated oil/water separation materials can achieve industrial-scale production and be put into use for oil spill and industrial oily water treatment in the near future.

1. Introduction

The leakage of oil in ocean is a big catastrophe in the world which will bring many toxic compounds to the ocean and thus threaten every species along with the marine food chain, from low grade algae to higher mammals even including human beings.^{1,2} The historical oil spill accidents frequently occurred and never ended, from the 1967 Torrey Canyon oil spill to the latest 2011 Bohai Bay oil spill, making the oil spill urgently need to be addressed. In addition to the burning of oil, artificial separation of the oily water is a more favourite way since the spilled oil can be re-collected without causing environmental pollution and reused in various industries. The traditional oil/water separation technologies include gravity separation, filtration, centrifuge, flotation, electrochemical method and so forth³⁻⁵. However, most of the traditional oil water separation methods often take a long time and need tedious manual operation. Moreover, the separation process of oil-and-water mixture is empirical to a great extent, thus making the separation halfway with either oil remaining in water or water remaining in oil.

The rapid development of colloid and interface science and

bionics in the past decades, especially for the superhydrophobic surface⁶⁻¹³ and deuterogenic underwater superoleophobic surface¹⁴⁻¹⁷, has offered a bran-new idea for developing efficient, automated and recyclable oil/water separation materials that can thoroughly separate the water-and-oil mixture without exhausting any external energy. Compare to the traditional separation methods, the special wettability-controlled oil water separations show big advantages in both the separating speed and the efficiency of separation. As a type of special wettability, superhydrophobicity/superoleophobic is commonly defined as possessing a water/oil contact angle (CA) higher than 150° but a sliding angle less than 10° under a certain external environment.¹⁸⁻²² Superhydrophobic surfaces are of great interest in various applications, including self-cleaning windows/windshields²³⁻²⁶, anti-fouling²⁷, anti-dragmicrofluidic devices²⁸, oil/water separation materials and so forth²⁹⁻³¹. As the most widely applications, gravity driven oil/water separation material was first discovered by Jiang *et al.* in 2004 and further developed also by Jiang *et al.* in 2011, from the initial oil/water separation strategy that allows oil to permeate the as-prepared materials to more advanced strategy that allow water pass through the as-prepared materials. The interest in oil/water separation materials inspired by special wettability in the nature

from 2004 onwards has risen rapidly for all classes of substrates. Up to 2013, according to the literature retrieval in RSC, ACS, Wiley, Elsevier and Springer, there were in total about 5% records in 2004~2009, 6% records in 2010, 12% records in 2011, 19% records in 2012 and 58% records in 2013, denoting the rapid development in recent years. (Fig. 1). To utilize the special wettability to separate a water-and-oil mixture, the oil/water separation materials commonly possess an opposite wettability to water and oil. In general, oil/water separation materials can be created in two ways, either fabricating superhydrophobic/superoleophilic materials or developing superoleophobic/superhydrophilic materials in a definite external circumstance. The as-reported approaches commonly tend to prepare the former ones that can filter oils from water. Our group has prepared the superhydrophobic fabrics and sponges on which a series of transition metal nanocrystals (Fe, Co, Ni, Cu and Ag) coated by dip coating method³² and *in situ* growth method³³. In addition, our group also prepared hierarchical structured stainless steel mesh films/fabrics/sponges via the oxidative chemical polymerization of aniline³⁴ and hydrothermal method³⁵. The former method was more popular in the early studies, and the later was emerging till 2011 due to the difficulty in obtaining superoleophobic and superhydrophilic properties in air. Therefore, scientists ingeniously designed the underwater superoleophobic and superhydrophilic surfaces to realize oil/water separation via a simple pre-wetted process of the membranes.

In this feature article, we reviewed the latest researches on the field of oil/water separation stimulated from special surface wettability. Four typical materials with special wettability were specifically focused that can be applied for efficient separation of the common layered mixture of oil and water in Section 2, which in turn are superhydrophobic and superoleophilic materials (Section 2.1), superhydrophilic and under-water superoleophobic materials (Section 2.2), superhydrophilic and superoleophobic materials (Section 2.3), and smart materials with switchable wettability (Section 2.4). Particularly, in Section 3, the emerging materials with special wettability for oil/water emulsions separation were discussed. Next, the comprehensive understanding of all kinds of oil/water separation materials was put forward in Section 4. Moreover, theories related were proposed to understand the mechanisms of oil/water separation process for both in air and underwater (Section 5). Finally, conclusions about this review and outlook of this research on the future were proposed (Section 6).

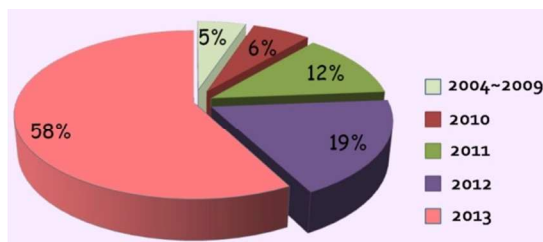


Fig. 1 The percentages of published papers about special wettability stimulated oil/water separation materials retrieved from the RSC, ACS, Wiley, Elsevier and Springer at 2004~2009, 2010, 2011, 2012 and 2013.

2. Separation of layered oil-and-water mixture

2.1 Superhydrophobic-superoleophilic materials

Superhydrophobic-superoleophilic materials are typical oil removing materials. The superhydrophobic and superoleophilic properties will make oil phase easily spread, absorbed (for porous bulk materials) and penetrate (for porous filter materials) on the material while the water phase will be repelled, thus separating oils from oil and water mixture. As is known, the surface wettability is determined by the combined effect of surface chemical composition and topography⁶⁻¹³. Accordingly, superhydrophobic-superoleophilic materials can be fabricated in two strategies: the first is to construct rough structure on hydrophobic surface; the second is to modify chemicals with low surface energy on rough surface.¹⁰ The ideal oil removing materials are generally considered to exhibit superhydrophobic and superoleophilic properties, high oil absorption capacity and low water pickup, low density, environmental friendly, self-propelled exhausting external energy, and good recyclability for a wide range of oils/organics. The prevailing oil removing materials are fabric-based materials, sponge-based materials, metallic mesh-based materials, carbon and its derived materials, and particles, which are discussed in detail in the following sections.

2.1.1 Metallic meshes based materials

Superhydrophobicity of a metal substrate has been intensely studied in the past decades³⁶⁻³⁹. To enhance the superhydrophobic and superoleophilic behaviour of a porous metallic mesh film, a filtering mesh with selective permeability to water and oil is prepared, resulting in oil/water separating property.

Stainless steel mesh was the first material for fabricating superhydrophobic and superoleophilic surface via a spray-and-dry method by Feng *et al.* in 2004 (Fig. 2a and b)⁴⁰. The pre-mixed aqueous emulsion containing teflon, adhesive (polyvinyl acetate), dispersant (polyvinyl alcohol), surfactant (sodium dodecyl benzene sulfonate) was sprayed on copper mesh evenly with compressed air and then underwent high-temperature drying process (350 °C) to decompose the adhesive, dispersant and surfactant. The prepared mesh is so water-repellent that the water droplet is unstable on such mesh and easily rolls off (Fig. 2c). However, oil spreads quickly on the mesh and permeates thoroughly within only 240 ms (Fig. 2d). It demonstrated that the as-prepared mesh could separate the mixture of diesel oil and water. Moreover, the results showed that the hydrophobicity of the coating mesh films was severely affected by the pore diameter of meshes. Since then, various methods and material coatings were employed to fabricate superhydrophobic and superoleophilic oil-water separation films, not only on stainless steel mesh substrates⁴¹⁻⁴⁴, but also on the other substrates which will be specially introduced in the following sections. Feng and his team⁴³ reported a polydopamine coated-stainless steel mesh with high hydrophobicity (the water CA of 144°) and superoleophilicity (the oil CA of 0°) through combining mussel-inspired chemistry (self-polymerization of dopamine at pH = 8.5) and Michal addition reaction of n-dodecyl mercaptan (NDM) with polydopamine (PDA). The as-prepared mesh could separate a series of oil/water mixtures like gasoline, diesel, etc. (Fig. 3) Meanwhile, the separation efficiency remained high (99.95% for hexane/water mixture, Fig. 3c) after 30 recycle numbers (Fig. 3d). More importantly, the relatively high intrusion pressure (2.2

Kpa) gave the opportunity to the separation of oil and water mixtures. Due to the easy oxidation of dopamine in air, the method is also applicable for other substrates such as fabric⁴⁵ and sponge⁴⁶.

In addition to stainless steel mesh, copper mesh was another most used substrate material for oil/water separation.⁴⁷⁻⁵² Lin *et al.*⁴⁹ reported a superhydrophobic and superoleophilic copper mesh through solution-immersion in HNO₃ solution and sequential modification with 1-hexadecanethiol. This as-prepared mesh could be used to separate the mixture of oil and water. Importantly, the superhydrophobicity of the mesh was stable even in corrosive environment, which enlarged the scope of application to some harsh aqueous environment. Moreover, other properties such as catalysis can be combined with the oil/water separation process. Feng *et al.*⁵⁰ reported a novel and multifunctional double-layer TiO₂-based copper mesh with superhydrophobicity and superoleophilicity, which could not only achieve oil/water separation but also degrade the organic pollutants in the water.

The surface modification with low surface energy materials is required for the vast majority of the mesh to fabricate superhydrophobic (or hydrophobic) and superoleophilic (or oleophilic) surface. However, secondary pollution might be produced by the modifiers, especially fluoride. Recently, the superhydrophobic (hydrophobic) and superoleophilic (oleophilic) stainless steel meshes were obtained in the absence of modification of low surface energy materials or fluorinated chemicals.⁵³⁻⁵⁶ Lee *et al.*⁵³ synthesized vertically-carbon nanotubes (vertically-CNTs) on a stainless steel mesh for the separation of oil and water. The dual-scale structure (with nano-scale needle-like tubes on the mesh with micro-scale pores) was coordinated with the low surface energy of carbon, resulting in both enhanced hydrophobicity and oleophilicity. The CAs for diesel and water were 0° and 163° ± 4°, respectively. Similarly, superhydrophobic and superoleophilic carbon nanotubes coated-stainless steel mesh was fabricated through thermal chemical vapour deposition for oil-water separation.⁵⁴ Very interestingly, the as-prepared mesh has the ability to dewater the water-oil emulsion. It is obvious that the modification by low surface energy materials without fluorine is more environmentally friendly since it decreased the usage of poisonous chemicals.

Except for the above two-dimensional meshes, recently, the three-dimensional (3D) metallic meshes were also reported.⁵⁷⁻⁶⁰ Sun *et al.*⁵⁷ described a simple approach for the fabrication of superwetting mesh films (SMFs) by using engineering commercially available stainless-steel grids based on a layer-by-layer grapheme assembly. Due to the good mechanical flexibility of the mesh, the SMFs can be simply folded or bent to prepare closed 3D-SMF for large-scale transportation. The cubic 3D-SMF could selectively absorb and stored the oils from oil-and-water mixture into its inner chamber. (Fig.4) Deng *et al.*⁵⁸ provided stainless steel mesh with hydrophobicity and oleophilicity for oil spill recovery devices by dip-coated in a xylene solution of low-density polyethylene. The wettability performance of 3D mesh was considerably improved in comparison to traditional oil/water separation technologies.

In short, various superhydrophobic and superoleophilic metallic meshes, including two-dimensional or three-dimensional meshes,

were successfully fabricated, which could be applied in efficient separation of the mixture of oil and water. However, there are some questions and challenges. First, the rough structure of these superhydrophobic and superoleophilic metallic meshes can be easily destroyed, which leads to the lose of superhydrophobicity and oil/water separation ability. Second, these superhydrophobic meshes cannot be applied to the in-situ oil removal since the oil-contaminated water must be firstly collected and then filtered, which are not suitable for the large scale of oil spill. Third, the vast majority of oils and organic solvents show smaller density than that of water. Thus, superhydrophobic-superoleophilic meshes are not suitable to the large-scale oil/water separation since floating of oils on water makes the oils hard to keep touch with mesh surface, resulting in low separation efficiency and speed. Fourth, so far, the metallic mesh films used for oil/water separation are mainly the stainless steel meshes and copper meshes, other kind of metallic meshes are seldom focused. Thus, the development of other kinds of metallic meshes should be also concerned since it may provide various choices facing the complex and specific environment.

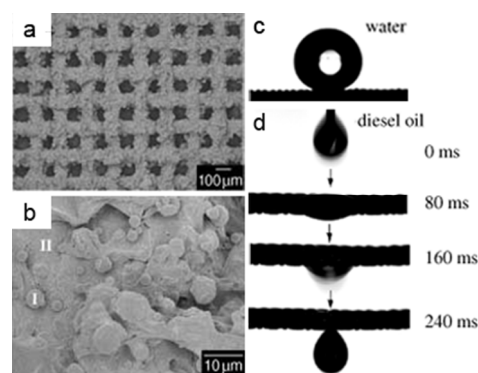


Fig. 2 (a) Scanning electron microscopy (SEM) images of the coating stainless steel mesh (average pore diameter is about 115 μm); (b) high-resolution view of (a). (c) Shape of a water droplet on the resultant mesh film with a water contact angle (WCA) of 156.2° ± 2.8°; (d) The diesel oil spreads and penetrates the copper mesh film quickly within only 240 ms, indicating a oil contact angle (OCA) of 0°. Reprinted with permission from ref.40. Copyright 2004 Wiley.

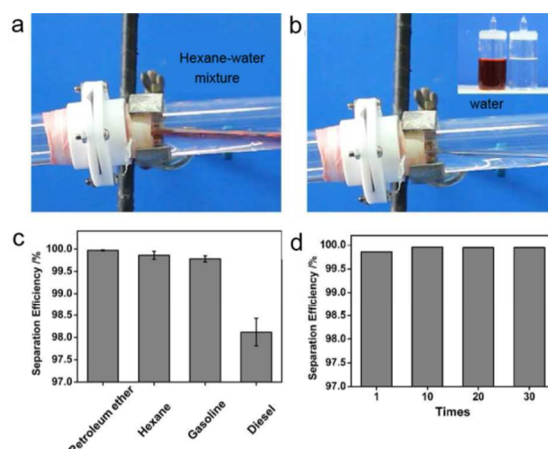


Fig. 3 (a - b) The process of oil/water separation based on highly hydrophobic PDA-NDM mesh. (c) The separation efficiency of the PDA-NDM mesh for a selection of oil and water. (d) Separation efficiency remains high after 30 times use by taking hexane as an example.

Reprinted with permission from ref.43. Copyright 2013 ACS.

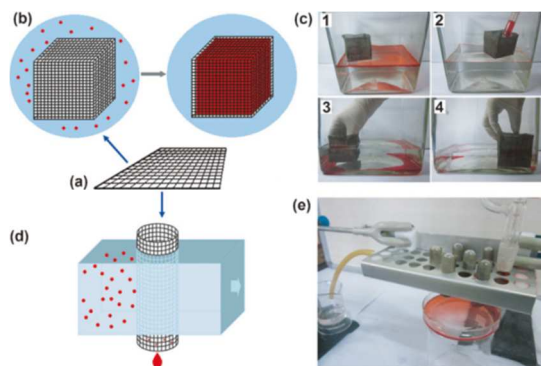


Fig.4 Sketch of a SMF. (b) Scheme illustrating a cubic 3D-SMF prepared from the SMF for selective absorption of an oil (red)/water (blue) mixture. (c) Snapshots demonstrating selective absorption of octane (1, 2) and chloroform (3, 4) from water by using a cubic ($6 \times 6 \times 6 \text{ cm}^3$). (d) Scheme illustrating a columnar 3D-SMF prepared from the SMF for oil (red)/water (blue) separation. (e) Equipment assembled used in (d) for chloroform/water separation, showing the water bypassed the columnar 3D-SMF whereas the chloroform was collected.⁵⁷ Reprinted with permission from ref.57. Copyright 2013 Wiley.

2.1.2 Fabrics based materials

Apart from inorganic porous metal films, fabric, a kind of soft and flexible organic material, is also considered as a good candidate for oil/water separation after various post-treatments since the ready-made fibres consisted of the integral fabric have provided the micro-scale roughness and the native porosity ensures the free passage of liquids. It commonly possesses intrinsic hydrophilic or unstable hydrophobic (the CA will gradually decrease during the penetration process of water) property due to the presence of oxygen groups. Till now, fabric has been popularly applied to construct various functional surfaces with special water (oil) wettability⁶¹, from the initial superhydrophobic fabric^{62,63} to the harder-to-achieved superoleophobic fabric and superomniphobic fabric^{64,65}.

To realize the separation of a mixture of water and oils or organics, establishing rough structured surfaces on fabric, with both superhydrophobic and superoleophilic properties, is a good choice. Dip coating procedure is the simplest approach and has been performed by many research groups⁶⁶⁻⁶⁸. Xue *et al.*⁶⁶ prepared the superhydrophobic cotton fabrics by immersing the pristine fabrics into the titania sol to generate a dual-size surface roughness and followed by hydrophobization with stearic acid. Wang *et al.*⁶⁷ presented a superhydrophobic cotton textile with oil/water separating property by dip coating superhydrophobic modified-ZnO/polystyrene nanocomposite coating. In addition to dip coating method, Ding *et al.*^{69,70} fabricated a superhydrophobic and superoleophilic nanofibrous membrane with oil/water separation property by the combination of electrospun poly(m-phenyleneisophthalamide) (PMIA) nanofibers and a novel *in situ* polymerized fluorinated polybenzoxazine (F-PBZ) functional layer that incorporated SiO₂ NPs. In addition, they⁷¹ reported a hydrophobic-oleophilic fibrous mat via co-axial electrospinning method where the polystyrene (PS) solution was used as the shell solution and polyurethane (PU) solution was used as the core solution. The prepared composite PU-PS fibrous mats showed

good oil absorbent capacity and excellent reusability. Other approaches such as chemical vapour deposition⁷², layer-by-layer technique⁷³, sol-gel method⁷⁴ and electro-spinning method⁷⁵ were also reported. Zhang and Seeger⁷² proposed a superhydrophobic and superoleophilic polyester textile by a one-step growth of silicone nanofilaments onto the textile via chemical vapour deposition of trichloromethylsilane. Compared with the original hydrophilic textile (Fig. 5a), the resultant textile was water repellent (Fig. 5b and c) and could be applied for oil/water separation in the form of filtration membrane. Frankly, fabric is not a good candidate for large-scale oil absorption owing to its thin, paper-like two-dimensional structure, which seriously limits its oil capture. However, the selective oil absorption ability of fabric was well performed by Zhang and Seeger⁷². To utilize the good flexibility and mechanical stability, the fabric was designed as a bag (Fig 5g) containing absorbent material. The fabric bag could function as selective oil absorption material, showing good separation efficiency and excellent reusability (Fig. 5g-k). Besides, some nonwoven materials can be also applied as the substrate material for oil/water separation due to their extremely similar microstructure with plenty of cross-linked fiber.⁷⁶

In addition, stability of the as-prepared superhydrophobic fabrics is also important since an excellent stability will endow the fabrics with more durable and robust properties, thus lengthening their lifetime and reducing production cost⁷⁷⁻⁸⁴. Zhang *et al.*⁷⁸⁻⁸⁰ presented a durable and robust superhydrophobic textile with good mechanical (e.g., abrasion, laundering, scratching with scalpel and adhesion of double side tape), chemical (e.g., exposure to acid and organic solvents) and environmental (e.g., exposure to UV irradiation and outdoor conditions) durability by simply dip-coating a nanocomposite solution of fluoro-free organosilanes. The as-prepared textile can be efficiently applied to separate oil-and-water mixture.⁷⁹ Zhang *et al.*⁸¹ reported a robust superhydrophobic cotton fabric that can withstand severe environment conditions such as high temperature (up to 120 °C), humid atmospheres (with a relative humidity up to 95%), corrosive substance, and mechanical forces (the water CA was higher than 150° and the separation efficiency remained above 93% after 600 times' scratch experiments) by *in situ* vapour phase deposition process. Otherwise, as-prepared fabrics can be effectively and sustainably used for oil-spill clean-up. Seeger *et al.*⁸² reported a simple one-step method to have the silicone nanofilament coated onto various fabric substrates. As-prepared fabrics show unparalleled long-term water resistance and stability of the superhydrophobicity that can maintain the superhydrophobicity even after continuous rubbing with a skin simulating friction partner under significant load. In our group, we proposed general methods to fabricated stable superhydrophobic fabrics via both dip coating⁸³ and chemical *in situ* growth⁸⁴ of transition metal/metal oxide nanocrystals (including Fe, Co, Ni, Cu and Ag) with n-octadecylthiol modification (Fig. 6a). The result showed that both the wettability and the coating capacity increase after the *in situ* growth of nanoparticles, which correlated positively with the concentration of the precursor. (Fig. 6b) As-prepared fabrics could be efficiently used to separate oil-and-water mixture (Fig. 6c). Interestingly, either the fabrics with different metal nanocrystals or the metal with different combined state (metal or metal oxide)

grown on them show different colours (Fig. 6a), which would enhance both their potential application and aesthetics.

In general, the developed superhydrophobic and superoleophilic fabrics by various physical and chemical routes, such as dip coating method, chemical *in situ* growth approach, electrospinning strategy and so forth, commonly can be applied to separate the water-and-oil mixtures with high separation efficiency. However, a major drawback existing on the substrates themselves (such as metal mesh film and fabric) is that the as-prepared materials cannot be directly used to deal with the oil spills on the ocean since they require the polluted water to be collected first and then filtered, which is inconvenient in the actual operation.

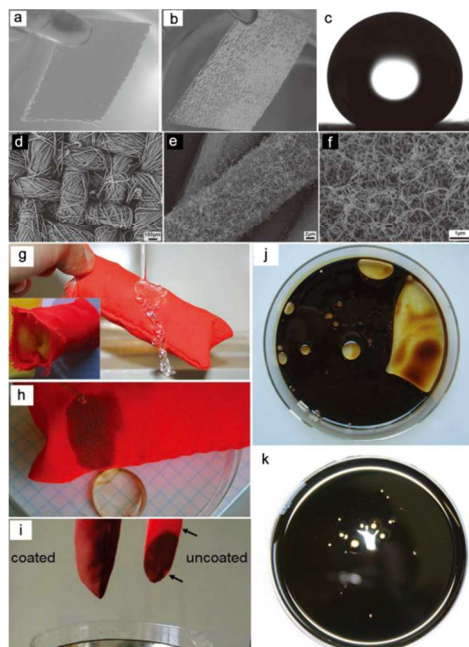


Fig. 5 Photographs of the pristine textile in water (a) and the resultant textile in water (b) for 8 weeks. The resultant textile is reflective underwater due to the existence of the air cushion between the textile and the water phase, denoting a good water repellent property. (c) CA image of the resultant textile. (d-f) SEM images at various magnification of the resultant textiles (relative humidity (RH) 35%). (g) Optical images of a water column bounce off the resultant fabric bag. (h) Selective absorption of crude oil from water. (i) Optical images of pristine and resultant fabric bags after oil absorption. (j) Oil absorbed by the pristine fabric bag. (k) Oil absorbed by the resultant fabric bag.⁷² Reprinted with permission from ref.72. Copyright 2011 Wiley.

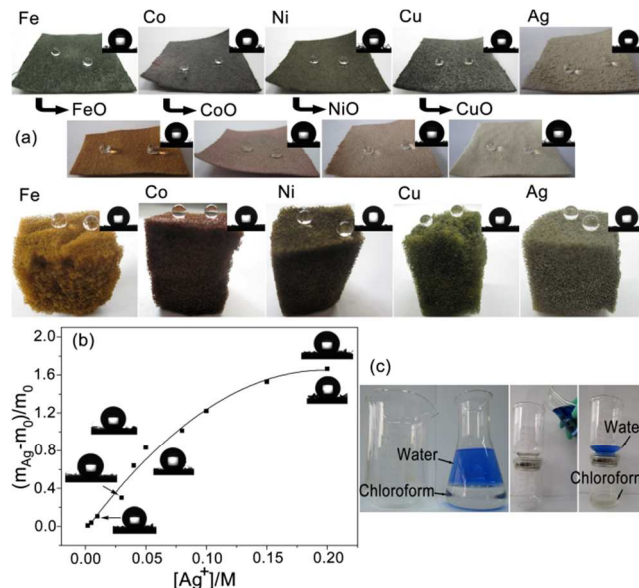


Fig. 6 (a) Optical images of superhydrophobic fabric/sponge from the *in situ* growth of Group VIII and IB metal/metal oxide nanoparticles. The inset images in the upper right-hand corner of each panel are images of the static water droplets (5 μ L) (b) Relationship between the proportion of weight increase (($m_{Ag} - m_0$)/ m_0) and the Ag^+ concentration. The images of CA modified with both n-octadecylthiol (upper left) and perfluorodecanethiol (lower right) at different concentrations are presented near the curve. (c) Photographs of the fabric-based oil/water separation process of water and chloroform. The water was dyed with Methylene Blue for clear observation.⁸⁴ Reprinted with permission from ref.84. Copyright 2013 ACS.

2.1.3 Sponges and foams based materials

Sponge and foam are cheap and commercial available porous materials with initial wettable property. Usually they can absorb various liquids (including water and oils or organics), which makes them unrealistic for removing oils/organics from water phase because of their poor selectivity. However, high selective absorption can be realized on a sponge after a purposeful construction of befitting surface topography and modification with low surface energy substance. It is one of the promising routes for developing oil/water separation materials. As with fabric, there are many oxygen groups inside and outside the sponge, making it hydrophilic or unstable hydrophobic. A vast majority of the methods used to prepare superhydrophobic fabrics are also applicable for sponges, such as *in situ* growth method^{45,84}, dip coating method⁷⁵⁻⁸⁸ and block copolymer (BCP) grafting strategy⁸⁹. Tai *et al.*⁸⁶ used the facile dip coating method to fabricate grapheme-based sponges with superhydrophobic and superoleophilic properties. Similarly, Li *et al.*⁸⁷ proposed a conjugated micro-porous polymer coated sponge with superhydrophobic and superoleophilic properties for facile and efficient separation of not only oils and nonpolar organic solvents but also those toxic or polar organic solvents from water. Pan *et al.*⁸⁸ used a solution-immersion process to prepare the superhydrophobic and superoleophilic PU sponges with Ag coating on them. Distinguished from fabrics, sponges and foams show the interconnected three-dimensional skeletons supported by chaotic fibre assemblies, thus endowing the sponges and foams with huge space for oil absorption and storage. Several

other approaches are also reported to fabricate rough structured superoleophobic/superoleophilic sponges that can be used as oil/water separation materials⁹⁰⁻⁹⁵. Choi *et al.*⁹⁰ prepared a polydimethylsiloxane (PDMS) sponge using a novel sugar-templating process. The resultant porous and elastic PDMS sponge showed high hydrophobicity and strong oleophilicity without any further surface modification. Zhang *et al.*⁹¹ applied a facile vapour-phase polymerization to fabricate superoleophobic and superoleophilic sponge using commercial PU sponges. Jiang *et al.*⁹² fabricated a superhydrophobic and superoleophilic sponge with oil removing property via deposition of polytetrafluoroethylene (PTFE) and two-time dip coating of amine-functionalized SiO₂ and SiO₂ particles followed by silane (octyltrichlorosilane) modification through vapour phase deposition process. They also⁹³ developed a chemical etching method to make the PU sponges immersed in a chromic acid solution and followed by surface modification with fluoroalkylsilane. Superhydrophobic sponges with a similar method were also reported by Pan *et al.* (Fig. 7a-e)⁹⁴. As a result, the resultant sponges showed good self-cleaning property (Fig. 7f). Furthermore, as-prepared sponges possessed durable acid and base resistant properties (Fig. 7g).

Except for the frequently mentioned resistant property to corrosive liquid, some other properties were also researched on the sponges/foams to realize the “multifunctional integration” which was first suggested by Jiang *et al.*⁹⁶. Therein, the most concerned property above all is magnetism^{97,98}. Calcagnile *et al.*⁹⁷ presented a composite magnetic material with highly efficient oil/water separation capability. They used a facile and easy scalable fabrication technique based on commercially available PU foams functionalized with colloidal superparamagnetic iron oxide nanoparticles and submicrometer CNT particles. After the separation procedure, the foam could be easily collected by a magnet (Fig. 7h and i). In addition to magnetism, conductivity is also considered by scientists, mainly based on carbon-coated sponge. Jiang *et al.*⁹⁹ reported a novel strategy for the fabrication of ordered and flexible polymer-based graphene foams (PGFs) by self-assembly of graphene sheets on the 3D skeleton of PU foam. The as-obtained PGFs possessed polymer skeleton, which effectively supported graphene foams, exhibiting high conductivity, hydrophobicity, outstanding mechanical properties, and excellent recyclability. Thereby, they could not only show considerable potential in oil/water separation field, but also be served as good candidate for pressure dependent resistor (Fig. 7j-l).

As the absorption efficiency of oils and organic solvents are commonly limited to the volume of air in the sponges/foams, some other strategies were suggested to fabricate superhydrophobic and superoleophilic sponges/foams with high absorption efficiency, in other words, with high porosity. Li *et al.*¹⁰⁰ proposed superhydrophobic activated carbon sponges by coating highly porous activated carbon particles onto sponge skeletons using a facile dip coating method, followed by PDMS treatment. The combination of highly porous activated carbon and the porous sponge skeleton endowed excellent absorption selectivity and absorbencies for various oils and organics. Moreover, a few sponge-templated carbon materials were developed by ultimately pyrolyzation of PU sponge but still

retained the sponge skeleton to form a simultaneous super porous and ultralight material.^{101,102} It is specifically discussed in next section (Section 2.1.4). The sponge/foam based superhydrophobic/superoleophilic materials show great potential for the direct and large-scale removal of organic contaminants or oil spills from water.

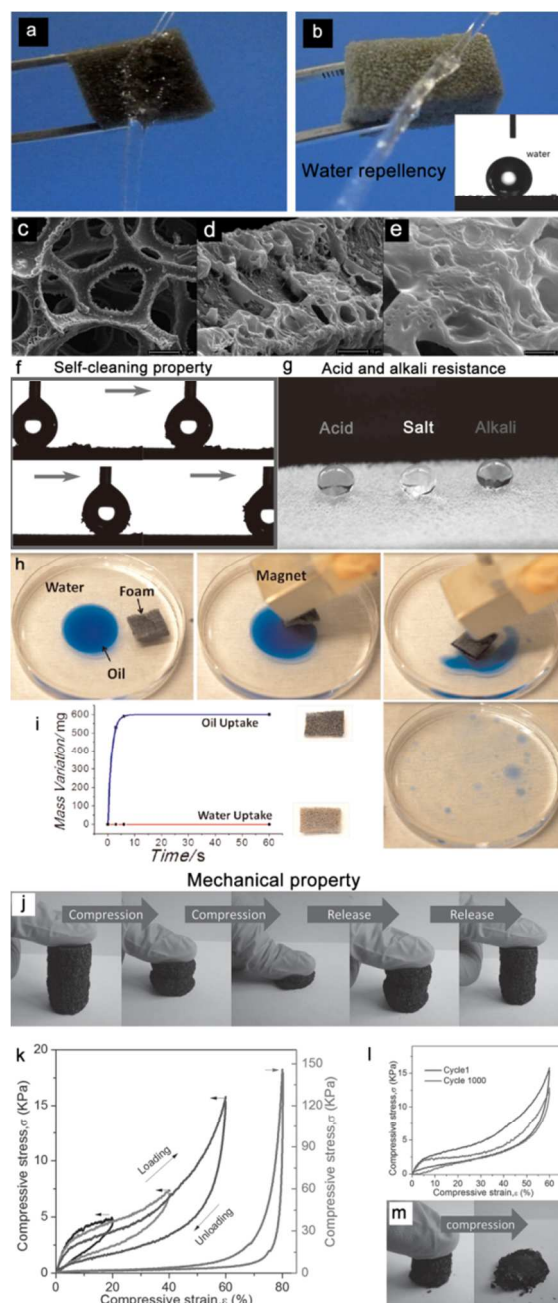


Fig. 7 Photographs of a water column squirted on a piece of pristine sponge (a) and superhydrophobic sponge (b).⁹⁴ The pristine sponge was immediately wetted by the water column whereas the superhydrophobic one strongly resisted the water column, indicating its water repellent property. (c-e) show the typical rough structured superhydrophobic sponge from an integral view (c) to the enlarged views (d, e)⁹⁴. (f) Demonstration of the self-cleaning property of the superhydrophobic PU foam via the removing process of carbon black particles from the surface using a moving water droplet (5 μ L).⁹³ (g) Demonstration of the corrosive liquids resistant property of the superhydrophobic PU foam by dropping aqueous hydrochloric acid (pH = 1), NaCl (pH = 7), and NaOH (pH = 14)

solution droplets with spherical shapes on the superhydrophobic PU foam.⁹³(h) Magnetically driven floating foams for the removal of oil contaminants from water.⁹⁷(i) Graph showing the variation of the weight of the foam with time.⁹⁷ (j-m) show the mechanical properties of PGFs with 6% graphene sheets. (j) Optical images showing the compression recovery process that PGFs recover their original shape after compression by more than 90%.⁹⁹(k) Stress-strain curves of PGFs with different set strain of 20, 40, 60 and 80%, respectively. (l) Cyclic stress-strain curves of PGFs at 60% strain at the compression speed of 10 mm min⁻¹.⁹⁹ (m) The compression-recovery process of graphene foam obtained by direct reduction of GO, and it collapses after a compression by 50%.⁹⁹ Reprinted with permission from ref.93, ref. 99. Copyright 2013 Wiley; reprinted with permission from ref. 94. Copyright 2013 RSC.

15

2.1.4 Carbon and its derived materials

Carbon-based aerogels, which are made up of interconnected three-dimensional networks, have intrigued huge condensation due to their outstanding properties, such as low density, high porosity, excellent electrical conductivity, large specific surface area, good chemical inertness and flexibility. As a result, carbon-based aerogels show enormous potential applications in supercapacitors, catalyst supports and so forth. In particular, their low density, high porosity and intrinsic hydrophobicity make them good candidates as the oil removing materials in the field of oil/water separation. In general, four kinds of methods are applied to obtain carbon-based aerogels, i.e. template method, freeze-drying method, chemical vapour deposition and pyrolysis method.

Template method usually applies self-supported porous materials or particles as the template. The template will be removed after target materials were prepared. According to the post-treatment of removing the template, two types can be classified: etching method and pyrolysis method. The resultant carbon material possesses hollow structure with only carbon skeleton retained. Koratkaret *et al.*¹⁰¹ proposed a 3D graphene foam network by applying porous nickel foam as template for deposition of graphene. After modification with teflon, the graphene foam became superhydrophobic with an advancing WCA of ~163° while the receding WCA is ~143°. Chen *et al.*¹⁰² fabricated a 3D graphene-CNT hybrid foam from chemical vapour deposition of graphene on nickel foam and subsequently *in situ* growth of CNT forest on it, followed by acid etching to remove nickel skeleton. The low-density hybrid foam can be efficiently applied as selective absorbent to remove oils and organic solvents from water. Li *et al.*¹⁰³ synthesized a mesoporous graphene by employing CaCO₃ microspheres as hard templates and PDMS as the modifier. The prepared mesoporous graphene prepared showed abundant mesopores which were crucial for realizing high absorption capacity and exhibited excellent separation ability for various organic compounds from water.

Particularly, pyrolysis method, as one type of template methods, is the most widely used by researchers^{104,105}. Sun *et al.*¹⁰⁶ fabricated twisted carbon fibers (TCF) aerogels from a facile pyrolysis method under argon gas atmosphere using the economic raw cotton. The TCF aerogels could absorb a wide range of organic solvents and oils (of 50–190 times of the weight of pristine TCFs aerogel) and exhibited excellent recyclability. Similarly, Yu *et al.*¹⁰⁷ reported a facile pyrolysis route to fabricate

ultralight, flexible and fire-resistance carbon nanofiber aerogels in large scale from bacterial cellulose pellicles. As-prepared carbon nanofiber aerogels showed excellent recyclability and selectivity for a wide range of organic solvents and oils (reach up to 310 times the weight of the pristine carbon nanofiber aerogels). They also¹⁰⁸ reported PDMS-coated carbonaceous nano-fibre hydrogels and aerogels which can be used as oil removing material and cycled by direct burning process via template-directed hydrothermal carbonization process. Generally, the pyrolyzation treated carbon-based materials can be divided into two kinds based on the elasticity, namely, flexible and inflexible. This makes a great difference on the oil reusability way since the flexible carbon-based aerogels can use a direct squeezing method, a combustion method and the distillation method to recycle the materials^{106,109}. However, the squeezing method is inapplicable for an inflexible carbon material. On the contrary, in order to recycle the oils or organics, the distillation method (Fig. 8h and i)¹¹⁰ is applicable to replace the squeezing method (Fig. 8e in 106).

Freeze-drying method usually use the directly sublimation effect of the as-prepared carbon hydrogel to obtain the carbon aerogel¹⁰⁹⁻¹¹⁴. It is a frequently used approach to fabricate carbon aerogel with large specific area and porosity. Sun *et al.*¹¹⁰ prepared spongy graphene by reducing a suspension of graphene oxide (GO) platelets and then moulding via a hydrothermal treatment and freeze-drying process. As-obtained spongy graphene showed well oil removing ability to petroleum products, fats, alkanes, toluene, and other organic solvents without any further modification or treatment (of 20~86 times the weight of the pristine spongy graphene) and could be repeatedly applied to removing oils by heat treatment to remove and collect the as-absorbed oils (Fig. 8i). Likewise, They¹¹¹ fabricated three kinds of porous reduced GO foams with different pore structures by the freeze-drying methods, i.e. unidirectional freezing drying, non-directional freezing drying, and air freezing drying. Gao *et al.*¹⁰⁹ fabricated all carbon ultra-flyweight aerogels (UFAs) by freeze-drying aqueous solution of CNTs and giant GO sheets, followed by chemical reduction to transform giant GO into graphene with hydrazine vapour. The prepared aerogels were purely made with carbon and showed extremely low density (the density $\rho \geq 0.16$ mg cm⁻³ and can even stand on a flower like dog's tail (Fig. 8a), temperature-invariant super recyclable compressibility and elasticity-responsive conductivity. Importantly, the hydrophobic carbon aerogels had a porosity (Fig. 8b) of ~99.9% and provided ultra-high oil-absorption capacity (of 215~913 times of the weight of pristine carbon aerogel). More importantly, to use the elasticity-responsive conductivity, this material could be used as pressure sensitive resistor (Fig. 8c and d). Qu *et al.*¹¹² developed a versatile, N-doped, ultralight 3D graphene framework with fire-resistant property and ultra-low density of 2.1 ± 0.3 mg·cm⁻³, which is the lowest to date for a graphene architecture. The graphene framework exhibited a very high capacity for the reversible adsorption of oils and organic solvents (of 200~600 times the weight of the pristine graphene framework) and could be easily recycled for many times.

Chemical vapour deposition (CVD) is also suggested to fabricate the porous carbon materials. Gui *et al.*¹¹⁵⁻¹¹⁷ reported sponge-like bulk material composed with self-assembled, interconnected CNT skeletons with ultralow density, a porosity of

> 99%, high structural flexibility and robustness, and it was wettable to organics in pristine form. It effortlessly floated on water surface and could quickly remove a spreading oil film on water with high efficiency (up to 180 times the weight of the pristine carbon nano-fibre aerogels). In addition, porous carbon materials can be also deposited on other substrate materials via CVD. Moon *et al.*¹¹⁸ used a glow discharge deposition process to fabricate carbon NP networks with tunable wettability and absorbability on various substrates such as silicon wafer, metals, paper and polymers.

Similar to the magnetic sponges/foams introduced in the previous section, the magnetic carbon-based materials were also developed to endow the maneuver ability and thus improve the practical applications. Pan *et al.*¹¹⁹ fabricated ultralight magnetic $\text{Fe}_2\text{O}_3/\text{C}$, Co/C , and Ni/C foams in centimeter scale by pyrolyzing PU sponge which was grafted with polyelectrolyte layers at 400 °C with the corresponding metal acrylate, forming the ultralight foams consisted of 3D interconnected hollow tubes. After the siloxane modification, the foams can be used to separate oils from water with a much higher oil-absorption capabilities than many other porous materials. Meanwhile, a three-dimensional macroporous Fe/C nanocomposite was also reported as the highly selective absorption materials for removing oils from water surface by sintering a mixture of closely packed polystyrene microspheres and ferric nitrate precursor.¹²⁰ The resultant nanocomposites exhibited superhydrophobic and superoleophilic properties without modification of low-surface-energy reagents. By applying a same method with ref 115 in addition to increase the concentration of ferrocene, a magnetic CNT sponge with rough porous structure consisting of interconnected CNTs with rich Fe encapsulated in it was obtained by Gui *et al.*¹²¹ The obtained magnetic CNT sponge showed application as sorbents for spilled oil recovery with high mass sorption capacity (up to 56 g/g) and excellent recyclability (more than 1000 times).

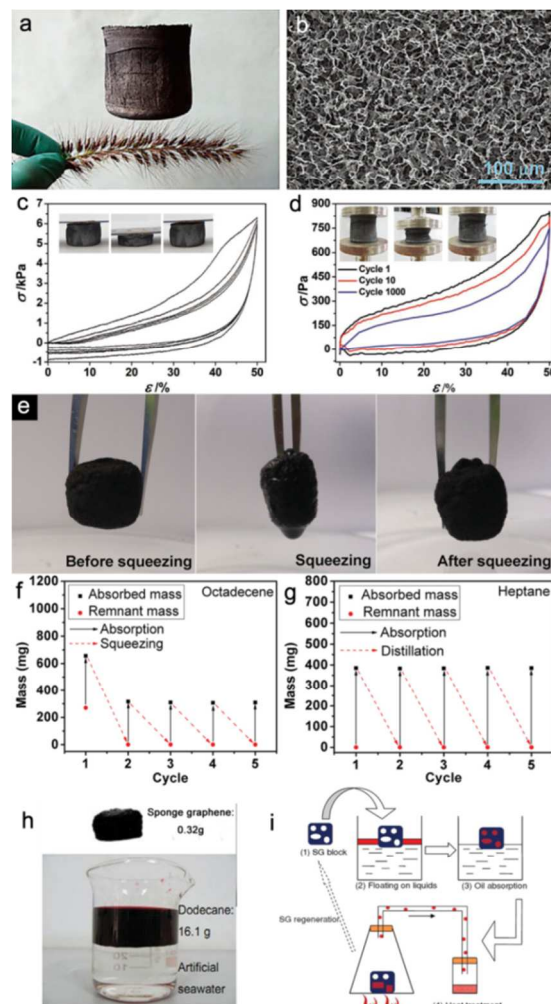


Fig. 8 (a) Digital photograph of a 100 cm³ UFA cylinder standing on a flower-like dog's tail (*Setairaviridis* (L.) Beauv), denoting the ultra-flyweight property of the UFA.¹⁰⁹ (b) SEM image of the porous architecture of a UFA.¹⁰⁹ (c) Stress-strain (σ - ϵ) curves of multicycle compression on a UFA ($\rho = 5.6 \text{ mg cm}^{-3}$, $f = 0.5$), exhibiting recoverable deformation. The inset shows the optical images of the UFA under a compressing and releasing cycle. The top head of the UFA was shuttling between a set fixed distance during the compression at a speed of 2 mm/min.¹⁰⁹ (d) Stress-strain curves of several selected cycles (the 1st, 10th, and 1000th cycle) on a UFA ($r = 1 \text{ mg cm}^{-3}$, $f = 0.5$) during repeated compression. The inset shows the optical images of the UFA under fatigue test for 1000 cycles. The compression and release speed is 600 mm/min.¹⁰⁹ (e) Photographs showing the process of recycling TCF aerogel via squeezing process.¹⁰⁶ (f) The recyclability of the TCF aerogel for sorption of octadecene via squeezing way.¹⁰⁶ (g) The recyclability of the TCF aerogel for sorption of heptane via distillation approach.¹⁰⁶ (h) optical image shows the sorption of oil.¹¹⁰ (i) Four-step schematic diagram of distilled recycling process.¹¹⁰ The carbon-based aerogel can be regenerated and reused without affecting its performance when heated up to the temperature around the boiling point of absorbate. The as-evaporated liquid could be recollected elsewhere after a condensation procedure and the carbon-based aerogel was willing to be applied in the next cycle of absorption without any post-treatment.¹¹⁰ Reprinted with permission from ref.106, ref. 109, ref.110. Copyright 2012, 2013 Wiley.

2.1.5 Particles and powders materials

To date, the superhydrophobic and superoleophilic surfaces used to water-oil separation were mainly fabricated on the porous substrates, such as meshes, fabrics, membranes, and so on. These oil/water separation surfaces allow oil to penetrate through them

whereas resist water due to the negative capillary effects. Although they can efficiently separate the mixture of oil and water, they cannot in-situ and selectively remove oil from oil-water interface. The pre-collection procedure of oil and water mixture is necessary. Recently, some novel hydrophobic and oleophilic particles without porous skeletons like sponges and carbon aerogels have been developed to achieve in-situ and selectively separate oil from the oil/water mixture.¹²²⁻¹²⁸ For example, Arbatan *et al.*¹²² reported a superhydrophobic and oleophilic calcium carbonate powder that can separate oil from an oil-water mixture quickly. Akhavan *et al.*¹²³ presented the hydrophobic and oleophilic plasma polymer coated silica particles for petroleum hydrocarbon removal. Guo *et al.*¹²⁶ fabricated a hollow core/porous polysulfone microspheres with superhydrophobicity and superoleophilicity for the selective removal of oil from water. Meanwhile, the particles and powders can be easily functionalized onto sponges/foams, resulting in superhydrophobic bulk materials for oil/water separation^{129,130}.

Although these particles and powders can be used in oil spill clean-ups, they were difficult to transfer and reclaim. Naturally, magnetic particles/powders were developed to overcome the reclaiming problem because particles/powders with magnetism can be easily collected under an external magnetic field. Wang *et al.*¹³¹ reported a fabrication approach of papilla-like magnetic particles with dual-scale structure via thermal treatment of Fe microparticles (Fig. 9a and b). These particles were immersed in aqueous solution of lauric acid to modify the papilla-like particles (LA-papilla-like particles) with desired wettability. The LA-papilla-like particles-composed surface had a water CA as high as $164.5^\circ \pm 1.6^\circ$ (Fig. 9c), whereas CA of oil was close to 0° (Fig. 9d). As shown in Fig. 9e, the LA-papilla-like particles could absorb oils and were separated from the water by a magnetic field. Then these LA-papilla-like particles with absorbed oils were transferred into ethanol to release oils, which made the oil remover regenerable. Through the adsorption and desorption of oil and magnetic motion, the oil contaminants in water were completely removed and the LA-papilla-like particles were easily regenerated and then reused many times.

Apart from the homogeneous magnetic Fe microparticles, more of the works were focused on the composite magnetic particles/powders¹³²⁻¹³⁷. Zhu *et al.*¹³⁴ reported fast and selective removal of oils from water surface through core-shell $\text{Fe}_2\text{O}_3@\text{C}$ nanoparticles with highly hydrophobic and superoleophilic properties under a magnetic field. These nanoparticles could selectively absorb lubricating oil up to 3.8 times of the particles weight while completely repelling water. In particular, the nanoparticles showed unsinkable property under agitation conditions, good stability toward corrosive media, and excellent recyclability. Zhang *et al.*¹³⁵ presented superhydrophobic core-shell-satellite carbonyl iron/polydopamine/silver composite particles to separate oil phase from oil/water mixture and could easily transport via external magnet field. Meanwhile, they also found that an oil sphere could be spontaneously formed under water encapsulated by superhydrophobic magnetic particles under the external magnet field.

It is obvious that hydrophobic and oleophilic particles and powders can be effectively used to solve the large scale of severe water pollution arising by oil spills because they are portable

and can be used to selectively remove oil *in situ*. However, there are two shortages on this kind of materials, which become a crucial obstacle for the practical production and application. First, the oil absorption capacity of superhydrophobic and superoleophilic particles and powder is low. Second, most magnetic hydrophobic and oleophilic particles are easily destroyed in acid solution, resulting in the loss of the recoverability, even the superhydrophobicity.

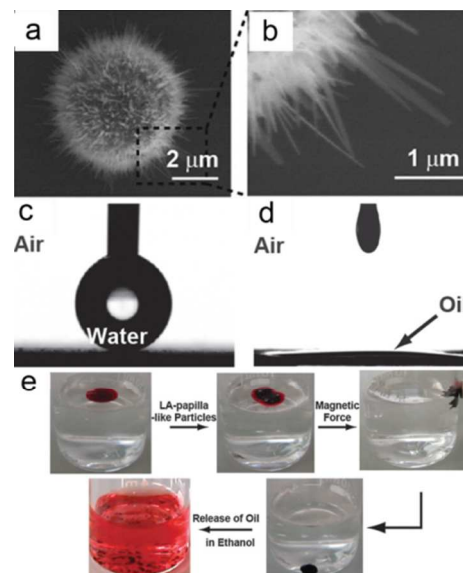


Fig. 9 SEM image of papilla-like particle; (b) enlarged view of nano-flake on papilla-like particle. Still photographs of a water droplet (c) and a corn oil droplet (d) residing on LA-papilla-like particles film. (e) Separation process of oil phase from oil-and-water mixture by using LA-papilla-like particles.¹³¹ Reprinted with permission from ref.131. Copyright 2013 RSC.

2.1.6 Other bulk materials

Aside from the substrates mentioned above, i.e. metallic meshes, fabrics, sponges, foams, particles/powders, and a few other bulk materials were also developed to realize oil/water separation¹³⁸. For example, a novel superhydrophobic CNTs-PTFE bulk material was prepared by Zhang *et al.*¹³⁹ The CNTs-PTFE bulk materials still showed excellent superhydrophobicity after 20 abrasion cycles and even after being deeply cut. This bulk material could be reused as oil sorbent in oil/water mixture. The oil-fouled bulk material could regenerate its superhydrophobicity again just by directly burning off the oil. Additionally, based on the CNTs-PTFE bulk material, they also obtained another kind of magnetic bulk material for easily removing oil from the water surface.¹⁴⁰ Hayase *et al.*¹⁴¹ presented a novel marshmallow-like macroporous methyltrimethoxysilane-dimethyldimethoxysilane (MTMS-DMDMS) gels that showed superhydrophobicity and could act as a sponge to remove organic compounds from water by absorbing them and then releasing them upon being squeezed out. The elastic properties were maintained over a wide temperature range, from the temperature of liquid nitrogen to 320°C. In addition, the introduction of different functional groups allowed for changing of the adsorption/absorption properties, which was advantageous in their use as separation media for different target compounds.

Interestingly, paper can be also applied as oil/water separation material just like the fabric.^{142,143} The superhydrophobic and

superoleophilic filter paper was successfully prepared by treating commercial filter paper with mixture of hydrophobic silica nanoparticles and polystyrene solution in toluene from Wang and coworkers. The SiO₂-coated filter paper could selectively adsorb oil that float on water surface or in aqueous emulsions. Interestingly, the filter paper could also extract from homogeneous aqueous solutions.¹⁴² The above-mentioned diversified substrates provide much more options to separate oil-and-water mixture.

Besides, most of the reported substrate materials are non-degradable, directly discarded or burnt after using, which will cause ground contaminants or create poisonous gases, accordingly resulting in secondary pollution to the environment.¹⁴⁴ To overcome the non-degradable property of the most reported substrates, Feng *et al.*¹⁴⁴ developed a biodegradable poly(lactic acid) oil absorption and filtration materials with superhydrophobic and superoleophilic properties via phase separation process. As-prepared materials can separate the oil and water mixture with high efficiency and easy recyclability. Meanwhile, the used materials can be easily decomposed because of their good biodegradable characteristic.

Moreover, the integral oil/water separation devices from the superhydrophobic and superoleophilic materials were also proposed¹⁴⁵⁻¹⁴⁷, which is significant and instructional for the industrial large-scale oil/water separation. Cheng *et al.*¹⁴⁵ reported a multifunctional device, which was fabricated by the superhydrophobic and superoleophilic nickel foam, for highly efficient and inexpensive oil spill clean-up. The device integrated the functions of oil containment booms, oil-sorption materials, oil skimmers, and water-oil separating devices. The device can be used for many types of oil/water mixtures, even for emulsion of petroleum and water, with high efficiency and reproducibility. Besides, they designed a functional integrated system with magnetically responsive to directionally absorb and continuously collect the spilled oil underwater, which demonstrated a re-collecting efficiency as high as 98%.¹⁴⁶

2.2. Superhydrophilic and underwater superoleophobic materials

As the vast majority of the oil/water separation materials are applied to allow the oil phase penetrate the surface (or absorb the oil phase) while repel the water, some scientists tried to exert their wisdom to develop the inverse oil/water separation materials that can let the water pass through freely however repel the oil totally. The fish scales, which are known to be well protected from contamination by oil pollution in the sea, have stimulated particularly consideration. Inspired by fish scales, the membranes with hydrophilic and underwater superoleophilic properties have been developed and shown great promising application as water-removing materials¹⁴⁸⁻¹⁵². This novel idea overcomes the defects that exist on the oil-removing materials, i.e., easily fouled or even blocked by the oils due to their intrinsic oleophilicity, thus limiting the recyclability. Moreover, the water removing materials avoided the formation of the water barrier between the substrates and the oil phase, which frequently occurred in the oil removing materials due to the fact that water commonly possesses a greater density than that of oils, thus preventing the contact between oil and separation substrates.¹⁵³ In addition, these materials will cause a waste of both the oils and the oil-removing

materials, especially for the oils with high viscosity. The as-absorbed oils were hard to clear away, which would easily cause a secondary pollution during the post-treatment of the materials.¹⁵⁴ In 2011, Jiang *et al.*¹⁵⁴ applied the hydrophilic polyacrylamide hydrogel-coated stainless steel mesh (Fig. 10a and b) to separate water from oil and water mixture after pre-wet up of as-prepared mesh before the oil/water separation process. The as-prepared mesh showed both underwater superoleophobic (Fig. 10c, d and f) and low oil-adhesion (Fig. 10e and f) characteristics in oil-water-solid three-phase system. The separation efficiency was above 99% for a series of oils, as given in Fig. 10g. This was the first oil/water separation material that allows water to pass through (Fig. 10h and i).

After that, based on the same principle, some researchers also proposed superhydrophilic and underwater superoleophobic materials via various methods^{153,155-159}. Yu *et al.*¹⁵⁶ reported an outstanding superhydrophilic and underwater superoleophobic film that can separate water from oil prepared by growing pure-silica zeolite crystals on stainless steel mesh. Wang *et al.*¹⁵³ proposed an all-inorganic-coating-based steel mesh via a layer-by-layer assembly strategy. The silicate/TiO₂ coated steel mesh showed superhydrophilic and underwater superoleophobic properties, which could be efficiently applied to separate water from oil phase. Meanwhile, as-coated TiO₂ showed UV-responsive property which endowed the mesh with degradative and self-cleaning ability. The mesh showed the equivalent functions with the double layer TiO₂-based mesh membrane fabricated by Feng *et al.*⁵⁰ however simplified the two separate meshes into one. Jin *et al.*¹⁵⁷ reported a superhydrophilic and underwater superoleophobic copper mesh film with ultralow adhesive superoleophobicity for water removing from oil-and-water mixture via facile chemical-based oxidation method. Besides, Feng *et al.*¹⁵⁸ used the one-step chemical oxidation of a smooth copper mesh to obtain a superhydrophilic and underwater superoleophobic Cu(OH)₂-covered mesh with hierarchical structure, which can selectively separate water from oil/water mixtures with high efficiency and excellent recyclability. Xu *et al.*¹⁵⁹ synthesized a biomineralized polypropylene/CaCO₃ composite nonwoven mesh by UV-induced poly(acrylic acid) grafting and alternate soaking process.

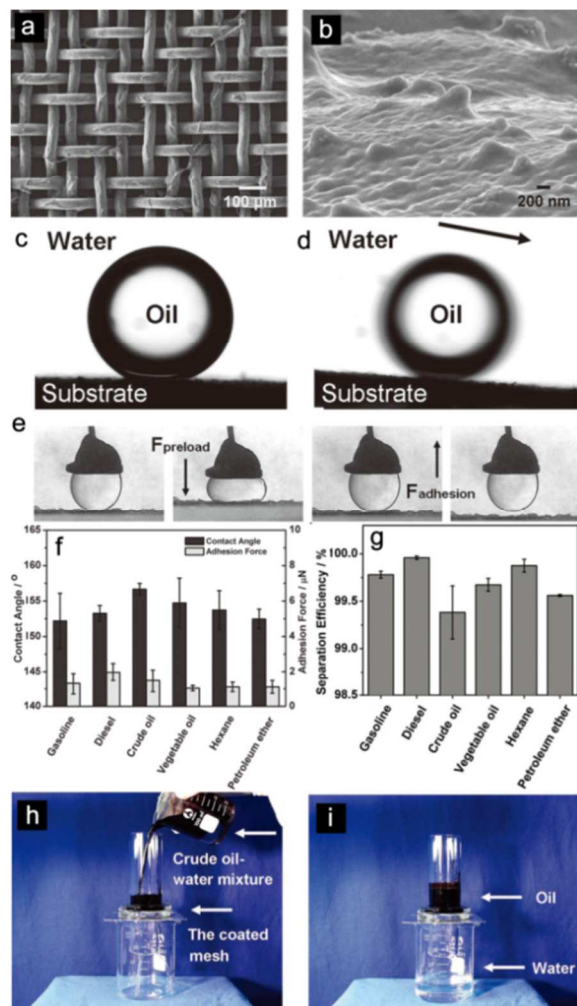


Fig. 10 SEM images of the polyacrylamide hydrogel-coated mesh prepared from a stainless steel mesh with an average pore diameter of about 50 μm . (a) shows the integral view and (b) shows the magnified view of one single wire on hydrogel-coated stainless steel mesh. (c) Still image shows the underwater oil droplet (1,2-dichloroethane, 2 μL) on the hydrogel-coated stainless steel mesh (OCA = $155.3^\circ \pm 1.8^\circ$). (d) Underwater sliding angle of oil droplet on the stainless steel mesh (oil sliding angle = $2.6^\circ \pm 0.5^\circ$). (e) Optical images of the dynamic underwater oil adhesion measurements on the mesh. A 5 μL oil droplet was applied as the detecting probe to contact the mesh surface and release. The mesh shows ultralow affinity to the water droplet. (f) Underwater oil wettability and oil adhesion of the resultant mesh for a series of oils in terms of CA and oil-adhesion force. (g) The oil/water separation efficiency of the resultant mesh for a selection of oils. (h, i) Oil/water separation process of the resultant mesh. The mesh film was fixed between two glass tubes. (h) Snapshot of the removal process of crude oil and water. (i) Snapshot after the removal process.¹⁵⁴ Reprinted with permission from ref.154. Copyright 2011 Wiley.

2.3. Superhydrophilic-superoleophobic materials.

In addition to the superhydrophilic and underwater superoleophobic materials introduced in the former section, another superhydrophilic and in-air superoleophobic material was developed that could also remove water phase from oil and water mixture and followed a quite different mechanism. Usually, a superhydrophilic (hydrophilic) surface exhibits superoleophilicity (oleophilicity) because oils commonly show lower surface free energy than water.^{160,161} And for a superoleophobic surface, it generally shows superhydrophobicity.¹⁶²⁻¹⁶⁴ However, a few

researchers find that some stimuli-responsive surfaces can simultaneously show hydrophilic and oleophobic properties based on a favourable interaction with polar liquids (e. g. water) and an unfavourable interaction with nonpolar liquids (e. g. hexadecane).¹⁶⁵⁻¹⁶⁷ To utilize the complexation of polyelectrolyte and oppositely charged surfactants, polyelectrolyte-fluorosurfactant complexes can be assembled on substrates. The stimuli-responsivity is caused the layer of polyelectrolyte-fluorosurfactant complexes that simultaneously contain hydrophilic (polyelectrolyte part) and oleophobic constituents (fluorosurfactant part). On these surfaces, oil is repellent by the surface because of the fluorosurfactant exposed outward. However, water is wettable because the interaction between polar water molecules and surface polyelectrolyte part can induce molecular rearrangement such that the hydrophilic moieties locate at the solid-liquid interface.

Although some moderate hydrophilic-oleophobic films have been reported¹⁶⁵⁻¹⁶⁷, extreme superhydrophilic-superoleophobic films are still challenges, and never been reported until 2012. To combine hydrophilic-oleophobic surfaces with a hierarchical rough structure, Zhang *et al.*¹⁶⁸ firstly fabricated poly(diallyldimethylammoniumchloride)-perfluorooctanoate/SiO₂(PDDA-PFO/SiO₂) coatings with simultaneous superhydrophilicity and superoleophobicity. The high surface concentration of fluorinated groups together with carboxyl and quaternary ammonium groups leads to a hydrophilic-oleophobic surface, whose mechanism is similar to the previous reports on the stimuli-responsive surfaces.¹⁶⁵⁻¹⁶⁷ Meanwhile, SiO₂ nanoparticles created micro- and nano-scaled hierarchical structures which could enhance the wettability to obtain superhydrophilicity-superoleophobicity (Fig. 11a and b). The PDDA-PFO/SiO₂-coated mesh with an average diameter of about 200 μm showed water permeation (Fig. 11c) and oil repellency (Fig. 11d) behaviors, which implied that the coated mesh could be applied to separate oil and water mixture. Moreover, the meshes could be cleaned with water and then dried for reuse.

In addition, a hygro-responsive membranes with both superhydrophilic and superoleophobic properties in air and under water were reported by Tuteja *et al.*¹⁶⁹. The membranes were fabricated by dip coating with fluorodecyl polyhedral oligomeric silsesquioxane (POSS) and cross-linked poly (ethylene glycol) diacrylate (x-PEGDA), forming the POSS + x-PEGDA complex. In air, the membrane surface is superoleophobic with several fluorodecyl POSS aggregates. While the membrane is immersed in aqueous environment, fluorodecyl POSS aggregates disappeared because of the surface reconfiguration caused by water molecules. The membrane could separate the oil-in-water emulsion (Fig. 12a and b) and the water-in-oil emulsion (Fig. 12d and e) by virtue of solely gravity-driven. The thermogravimetric analyses (TGA) analyses demonstrated that the separation efficiency was more than 99% (Fig. 12c).

The novel superhydrophilic and superoleophobic surfaces might be a good candidate in industrial oil-polluted water treatments, clean-up of oil spills, and fuel purification. However, the preparation methods of superhydrophilic-superoleophobic materials used to be complicated. To date, superhydrophilic-superoleophobic surfaces and their applications were still lack of

investigation, which remains a great challenge in their development.

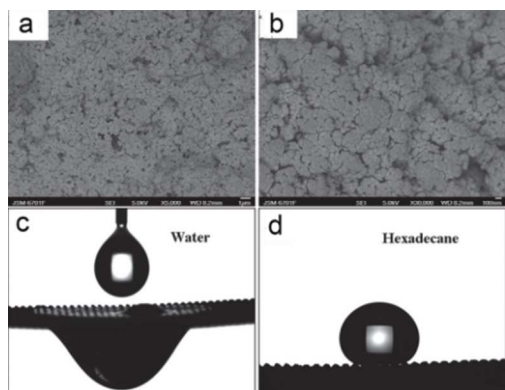


Fig. 11 (a) SEM images of the PDPA-PFO/SiO₂ coating showing a plenty of protrusions and pores on it. (b) Enlarged view of the coating. (c) Water droplet spreads and penetrates through the resultant mesh. (d) Shape of a hexadecane droplet on the mesh with aOCA of $157^\circ \pm 2^\circ$. The PDPA-PFO/SiO₂-coated mesh showed both superhydrophilicity and superoleophobicity.¹⁶⁸ Reprinted with permission from ref 168. Copyright 2012 RSC.

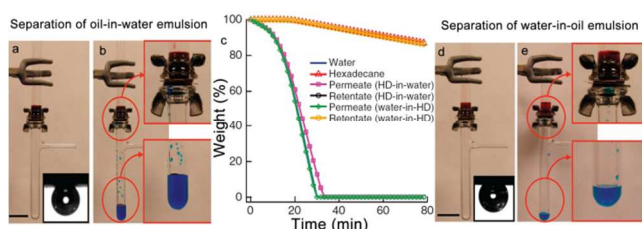


Fig. 12 (a, b) Photographs showing the separation of a 50:50 v:v hexadecane-in-water emulsion. Inset in (a) presents the wettability of underwater (with SDS of 1 mg/ml) hexadecane droplet on a surface spin-coated with a 20 wt% fluorodecyl POSS + x-PEGDA blend. (c) TGA data showing the permeates and the retentates. Therein, HD is short for hexadecane. (d, e) Separation process of a 30:70 v:v water-in-hexadecane emulsion. Inset in (d) presents the wettability of hexadecane droplet on a surface spin-coated with a 20 wt% fluorodecyl POSS + x-PEGDA blend.¹⁶⁹ Reprinted with permission from ref.169. Copyright 2013 NPG.

2.4. Smart materials with switchable wettability

Materials with stimuli-responsive wettability have attracted increasing interests because of their importance in fundamental study and industrial applications.^{170,171} These controllable surfaces wettability can be achieved by applying externally stimulus such as light illumination,¹⁷² temperature,¹⁷³ electrical potential,¹⁷⁴ and pH^{175,176} etc. Very recently, based on the extreme wettability switch, controllable oil/water separation materials have been developed, which has important significance on the treatment of oil contaminated water for different demand.^{89,177,178}

Polymers containing acid or basic functional groups usually possess pH-responsive wetting behaviour since their conformation and charges are dramatically influenced by the different pH solutions.¹⁷⁹ Based on this view, Zhang *et al.*⁸⁹ firstly developed smart materials that could be used for highly controllable oil/water separation processes. These smart materials with switchable superoleophilicity and superoleophobicity in aqueous media were prepared by grafting a BCP comprising pH-responsive poly (2-vinylpyridine) and oleophilic/hydrophobic polydimethylsiloxane (i. e. P2VP-*b*-PDMS) on commonly used

materials (Fig. 13a), such as textile (Fig. 13b and c) and sponges. Therein, the P2VP block could alter its wettability and conformation via protonation and deprotonation by changing the pH of the aqueous media, which provided controllable and switchable access of oil by PDMS block, resulting in the switchable surface oil wettability in the aqueous media (Fig.13f). Fig.13d and e showed the highly controllable oil/water separation processes by the resultant textile. When a mixture of gasoline and water with a pH of 6.5 was poured into the upper glass tube, the gasoline quickly passed through the textile membrane, but the water did not. However, when the textile membrane was first simply wetted by acidic water with a pH of 2.0 without subsequent drying and then under the same conditions, the opposite separation was realized, with water passing through the membrane this time. Unlike the above strategy, Guo *et al.*¹⁷⁷ adopted a mixture of carboxyl-terminated thiol and methyl-terminated thiol as a modifying agent on the hierarchical structured copper mesh to obtain pH-responsive mesh. The protonation and deprotonation process was controlled via altering the pH of aqueous media endowed controllable and switchable access of both oil and water by the apolar and polar thiol on the mesh, which resulted in the switchable surface in-air water wettability and underwater oil wettability. The as-prepared copper mesh had proved to be a smart material that could be applied to controllably and bidirectionally separate oil-water mixture.

Light is another widely reported external stimuli. Photo-responsive wettability switching between superhydrophobicity and superoleophilicity has ever been studied and reported.^{172,180} Recently, inspired by the extreme wettability switch, Zhai *et al.*¹⁷⁸ firstly reported photo-induced water-oil separation film, based on switchable superhydrophobicity-superoleophilicity and underwater superoleophobicity, an aligned ZnO nanorod array-coated stainless steel mesh was fabricated. The ZnO-coated mesh showed excellent controllability for separating different water-oil mixtures in an oil-water-solid three-phase system.

Thermal responsive was also developed to control the wettability of water on a solid surface in the early years. Poly(*N*-isopropylacrylamide) (PNIPAAm), as a thermal responsive polymer with a lower critical solution temperature (LCST) of about 32-33 °C, was applied to fabricate the surface with switchable wettability.¹⁷³ To utilize the thermal responsive polymer, Gao *et al.*¹⁸¹ reported a polymethylmethacrylate-*b*-PNIPAAm BCP with reversible switching between wettability states of hydrophilicity/oleophobicity and hydrophobicity/oleophilicity at different temperature. Namely, water could permeate the BCP-coated mesh, but oil could not when the temperature was below the LCST; however, oil could penetrate the mesh and water could not when the temperature was above the LCST. Therefore, this film offered promising applications in the controllable separation of water and oil mixtures.

Electric field is also developed by Tuteja *et al.*¹⁸² to switch the wettability and separate the oil/water mixture in a smart way. They developed the first-ever membrane-based single unit operation that could separate all types of oil-water mixtures with high separation efficiency upon applying a high electric field (higher than 1000 V).

On the basis of these strategies, functional materials with surfaces that have controlled water wettability (responsive to acidic or basic water) in air and oil wettability when submerged in an aqueous media, are expected to be used in many practical applications and help people designing and fabricating smart functionalized interfacial materials for both in-air and underwater applications. So far, there were a few reports with respect to the responsive materials for controllable oil/water separation. And, responsive materials only involved the pH-responsive materials, photo-responsive materials, thermally responsive materials and high electric field-responsive materials. Therefore, further research for controllable oil/water separation materials should be mainly focused on synthesizing new types of responsive materials, for instance, low electric field-responsive materials, stress-responsive materials, even dual- and multi-responsive materials.

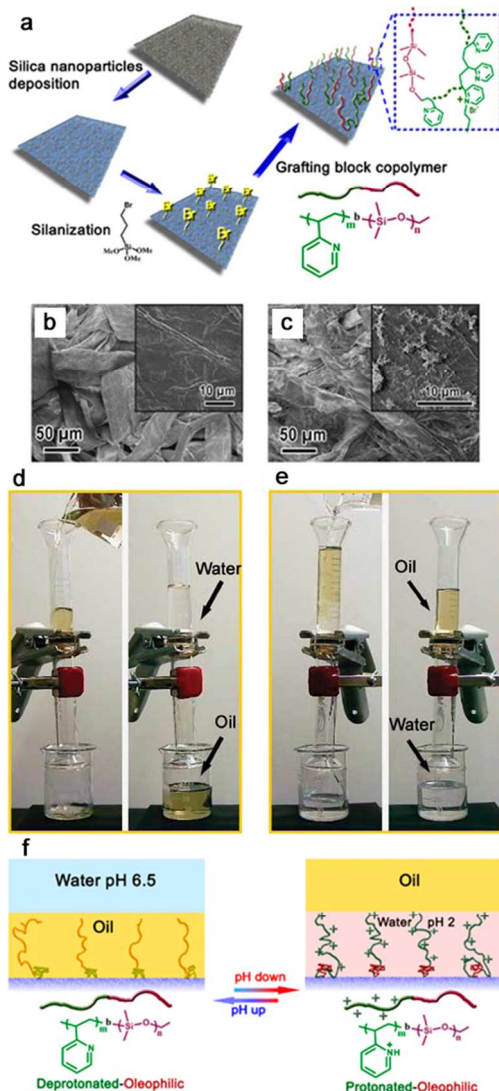


Fig.13 (a) Schematic illustration of the preparation procedure of a surface with switchable water and underwater oil wettability on a non-woven textile substrate. (b) and (c) show the SEM images of the raw textile and the textile after deposition of silica nanoparticles and BCP grafting. The insets in (b) and (c) show the enlarged view of single fibers. (d) and (e) show the controllable oil/water separation using the functionalized textile. (d) Separation of oil from the water phase. (e) Separation of

water from the oil phase. Therein, the functionalized textile was pre-wetted with acidic water (pH = 2.0). (f) Schematic diagrams for the switchable oil wettability of the P2VPb-PDMS-grafted textile.⁸⁹ Reprinted with permission from ref.89. Copyright 2012 NPG.

3. Separation of water-and-oil emulsions

As is known, the real oil/water mixtures are not always well layered. However, a large amount of oil/water mixtures to be processed, in fact, exist in form of emulsions. According to the report¹⁶⁹, an emulsion is defined as drop diameter of the dispersed phase is (water or oils) lower than 20 μm . The oils and water are generally considered as automatic layered in the most reported literatures since the oils and water are immiscible and their densities are different. Sometimes significant quantitative of hydrocarbons may be introduced into the water phase due to the solubility of light fractions (the solubility of hydrocarbons in water generally decreases as the carbon number increases¹⁸³), as well as the emulsification processes. At present, although porous materials with special wettability, such as superhydrophobic-superoleophilic and superhydrophilic-superoleophobic surfaces, have been applied to the separation of oil-water mixture, these materials are commonly not suitable for emulsified oil/water separation, especially for surfactant-stabilized emulsified, because the droplet sizes of the emulsion (usually less than 20 μm) are smaller than the pore sizes of these materials (\sim tens of micrometers). The emulsions separation materials can be also divided into the three kinds like the layered oil/water separation materials: superhydrophobic and superoleophilic materials, superhydrophilic and underwater superoleophobic materials, superhydrophilic and superoleophobic materials.

Jin *et al.*¹⁸⁴ prepared a superhydrophobic-superoleophilic poly(vinylidene fluoride) (PVDF) membrane, with a water CA of 158° and oil CA of less than 1°, by a facile modified-phase inversion approach (Fig. 14). As-prepared PVDF membrane was composed of spherical micro-particles and the individual micro-particles was isolated while being linked together through a fibre-like connection (Fig. 14a-c). This membrane could separate various water-in-oil emulsions including surfactant-free and surfactant-stabilized emulsions with droplet sizes from the micrometer to nano-meter range (Fig. 14d). Driven by gravity, the membrane exhibited high separation efficiency with > 99.95% oil purity after filtration and a high flux (Fig. 14e and f). It was worth noting that the membrane exhibited a good antifouling property, outstanding recyclability, thermal and mechanical stability and durability. In addition, they also reported a ultrathin single-walled CNT (SWCNT) for the ultrafast separation of emulsified oil/water mixtures.¹⁸⁵ As high permeation and nano-meter scale pore size were combined validly in the SWCNT films, a surprising flux of up to 100000 L m⁻² h⁻¹ bar⁻¹ and a high separation efficiency > 99.95 % were obtained. Tao *et al.*¹⁸⁶ presented a hierarchically hydrophobic porous silica monolith (HPSM) with macro- and meso-pores. The HPSM was synthesized by a sol-gel and phase separation process, subsequently modified by organic silanes. Oil droplets in a simple emulsion system (without emulsifier) were easily removed via filtration (Fig. 15a). In addition, when the emulsion was stabilized by surfactant, a “reverse membrane emulsification” process is often used, HPSM exhibited excellent demulsification ability via adsorbing the emulsifier from the emulsion, leading to

the completely broken of surfactant-stabilized emulsions. (Fig. 15b) The demulsification ratio reached 99.95% and the materials were reusable. Wang and co-workers¹⁸⁷ reported a robust superhydrophobic and superoleophilic CNT/poly (dimethylsiloxane)-coated PU sponge for the continuous absorption and expulsion of oils from water surfaces. Surprisingly, when been applied in conjunction with a vacuum system, this sponge could separate great amounts of oil up to 350000 times of its own weight and could also separate surfactant-free water-in-oil emulsions with high efficiency (oil purity: >99.97%).

Conversely, to separate the oil-in-water emulsion, a novel superhydrophilic and underwater superoleophobic zwitterionic polyelectrolyte grafted PVDF membrane was successfully fabricated by Jin *et al.*¹⁸⁸ through a surface-initiated atom transfer radical polymerization method. This membrane could thoroughly separate dispersed oil from water with ultrahigh separation efficiency (>99.999%), even the surfactant-stabilized oil-in-water emulsions with a droplet size in the micro-meter scale, however, it was not suit for emulsions with nano-meter-scale droplets because of the pore-size effect. Furthermore, due to the ultralow oil adhesion, the membrane showed an excellent antifouling property to oil and was easily recyclable. Afterwards, they reported¹⁸⁹ a salt-induced phase-inversion approach to fabricate poly-(acrylic acid)-grafted PVDF with superhydrophilic and underwater superoleophobic properties, showing big potential in separating oil-in-water emulsions with high separation efficiency and fluxes. Another work was suggested by Xu *et al.*¹⁹⁰, they reported a hydrophilization approach through co-deposition of mussel-inspired polydopamine and polyethyleneimine on polypropylene microfiltration membrane. The modified membranes exhibited good wettability and could be applied for oil-in-water emulsion separation.

In addition to the above superhydrophobic-superoleophilic and superhydrophilic-underwater superoleophobic materials, superhydrophilic-superoleophobic materials could also realize the separation of oil/water emulsion. Recently, Tuteja *et al.*¹⁶⁹ fabricated a POSS + x-PEGDA blend-coated hygro-responsive membranes with both superhydrophilic and superoleophobic properties in air and under water. This membrane could be employed in the separation of oil/water emulsion with droplet sizes larger than 1 μm with a separation efficiency $\geq 99.9\%$.

Membrane with special wettability have been demonstrated to be capable of overcoming the defects of the pressure-driven filtration membrane for oil/water emulsions.^{191,192} These defects mainly include the low flux and the quick decline in separation efficiency, which lead to a severe fouling issue and a clean-up problem.¹⁹³⁻¹⁹⁵ Therefore, it is expected that membrane with special wettability will replace the pressure-driven filtration membrane in the separation of oil-water emulsions.

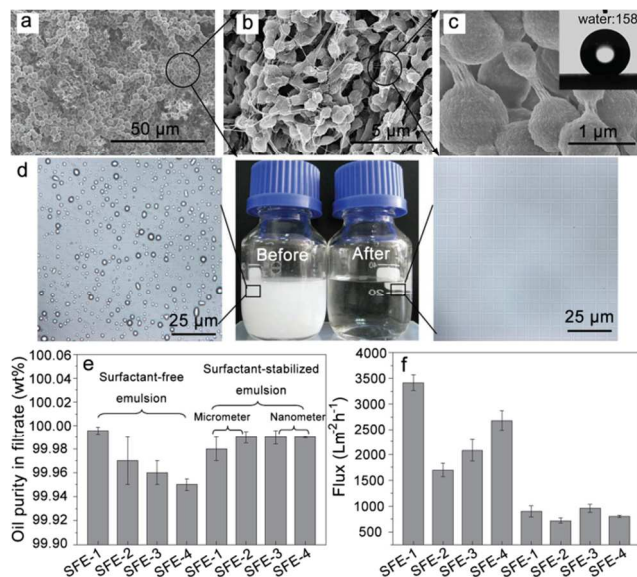


Fig. 14 (a - c) SEM images of PVDF membrane with different magnifications. The inset in (c) showed the image of a water droplet on the PVDF membrane (WCA = 158°). The drop sizes of the surfactant-free water-in-oil emulsions (SFE) were in the range of 5 – 20 μm . (d) Images of emulsion SFE-3 before and after filtration process. (e) Oil purity in the filtrate after penetration process via the PVDF membrane for a selection of emulsion. (f) Fluxes of a selection of emulsions when pass through the PVDF membrane. Therein, the labels SFE-1, SFE-2, SFE-3 and SFE-4 represent different kinds of oils, i.e. petroleum ether, toluene, isooctane, and dichloromethane in turn.¹⁸⁴ Reprinted with permission from ref.184. Copyright 2013 Wiley

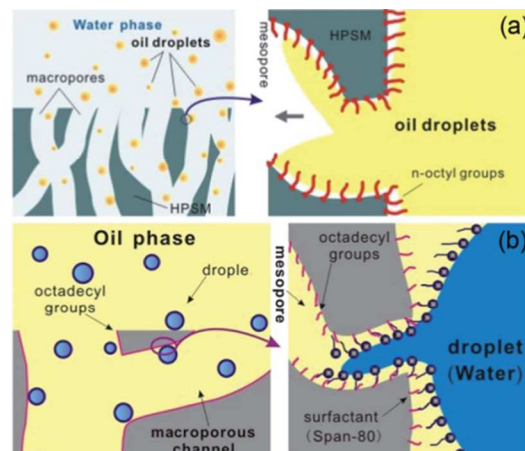


Figure 15 (a) A conjecture of the adsorption process of oils droplet by HPSM. When the oils droplet flowed through the macropore in aqueous environment, they could easily reach the inner pore surface and be absorbed into the mesopores. (b) The mechanism of the demulsification by HPSM. Firstly, the emulsifier-stabilized droplet was captured by the surface of HPSM. Then the micelle broke under the impact of flow. The surfactants remained on the silica surface and droplet was released. Finally, the unprotected small droplets got together and formed another continuous phase.¹⁸⁶ Reprinted with permission from ref.186. Copyright 2013 RSC.

4. Comprehensive understanding of all kinds of oil/water separation materials

As wide types of oil/water separation materials are specifically discussed in the former sections, here, the comprehensive understanding and comparison of these materials are also

proposed to acquaint the advantageous and disadvantages. Table 1 shows some typical oil/water separation materials depending on as-introduced substrates in the former sections. From the table, the oil/water separation features of all kinds of materials can be systematically understood, including substrate materials, preparation methods, wettability of water and oils, separation or absorption substances, separation efficiency of film-like material, absorption capacities of bulk materials, recyclability, cost, environmental protection. Meanwhile, separation efficiency of film-like material and absorption capacities of bulk materials are commonly the mostly concerned.

The separation efficiency is generally concerned in the film-like materials such as metallic mesh films and fabrics (sometimes sponge). The separation efficiency could generally reach > 90% for all kinds of films in the reported works (Table 1). Particularly, the membranes for the separation of emulsions could reach obvious higher separation efficiency due to the smaller pores on the membranes.

As for the absorption capacities, it is obvious that the hydrophobic particles and powders generally possess the lowest oil absorption capacities within several times of its initial weight. But for the superhydrophobic sponges/foams, the oil absorption capacities are much larger than that of the particles and powders, ranging from a dozen times to dozens of times when compared with the weight of original materials. The carbon-based aerogels generally show the largest oil absorption capacities. The oil absorption capacities could commonly reach over 100 times of the unused materials and the highest one could even arrive at 750 times of the unused material¹⁰⁹. The carbon-based aerogels is the most suitable one for oil removing in the view of oil absorption capacity. However, the preparation methods were usually complicate and the costs were usually expensive than those for the superhydrophobic sponges.

5. Theories behind the oil/water separation behaviour

5.1 In-air Contact Angle

The oil/water separation, in essence, is the wettability behaviour that occurs at the interface of solid, air, water and oil phase. When a liquid droplet was presented on an ideal smooth solid surface in air (Fig. 16a), the CA is determined by Young's equation¹⁹⁶

$$\cos\theta_0 = (\gamma_{SA} - \gamma_{SW})/\gamma_{WA} \quad (1)$$

where θ_0 is the Young's CA on the solid surface, γ_{SA} and γ_{WA} are the surface energies (surface tension) of the solid and liquid against air respectively, γ_{SW} is the interface energy (interface tension) between the solid and liquid. When it comes to a rough surface, two kinds of wetting states will occur, i. e., homogeneous wetting (Fig. 16b) and heterogeneous/composite wetting (Fig. 16c). While the homogenous wetting state happened, the CA of a water droplet could be given by the Wenzel equation¹⁹⁷

$$\cos\theta_W = r\cos\theta_0 \quad (2)$$

where r ($r > 1$) is the surface roughness factor defined as the ratio of the true surface area of the solid to its horizontal projection. From the equation, it can be observed that the apparent CA is determined by the combined effect of surface morphology (reflected by r) and surface chemical composition (reflected by

θ_0). While the surface chemical composition is fixed for a solid, the roughness can magnify the wettability levels of the solid surface to their extreme, either superhydrophilicity or superhydrophobicity. However, while the composite wetting state occurred, commonly with air trapped under the droplet, forming a solid-water-air wetting, the apparent CA (θ_{CB}) could be given by Cassie equation¹⁹⁸

$$\cos\theta_{CB} = r_f f_{SW} \cos\theta_0 + f_{SW} - 1 \quad (3)$$

where f_{SW} represents the solid-water fraction under the contact area. Distinguished from total roughness factor r , r_f is defined as the roughness ratio of the wet part of the solid surface and it always shows a lower value than r . Besides r , the Cassie equation suggests that the solid-water fraction (solid-air fraction) is also an influence parameter to the apparent CA.

5.2 Contact angle hysteresis and sliding angle

An oil/water separation material is either hydrophobic or oleophobic so that it can repel one phase of liquid while allow the other one permeate through it. To investigate hydrophobic and oleophobic surfaces, contact angle hysteresis (CAH) is another important concept that reflect the surface heterogeneity.^{10,199} The contact angle hysteresis is quite common on rough and chemical heterogeneous surfaces. In these cases, a series of apparent static CA can be observed, the maximum is called advancing CA and the minimum is called the receding CA. The CAH is generally considered as the difference between advancing CA and receding CA. Sliding angle (SA), the threshold tilting value of angle between the surface and horizon line, below which a liquid droplet start to roll/slide upon elevating an end of the surface. The SA decrease with the decrease of CAH. However, SA is not equal to the difference advancing CA and receding CA. Usually, superhydrophobic property means not only big static CA but also small CAH since the small CAH is responsible for the surface self-cleaning effect. Thus, CAH and sliding angle are also important indexes for the characterization of a super-lyophobic surface. For the two wetting states introduced above, Cassie wetting state commonly possesses both high CA and small CAH due to the air trapped below reduced the sliding resistance.

5.3 Transition between Wenzel and Cassie states

As shown in eqns (2) and (3), both the Wenzel relation and the Cassie relation give the information that the surface roughness can increase the surface hydrophobicity. Compared with Wenzel equation (eqn(2)), the Cassie equation allows for the possibility of the apparent CA lager than 90°, even with $\theta_0 < 90^\circ$. From the view of thermodynamics and energy barrier, the Wenzel and Cassie state are considered to be two separated energy minima with an energy barrier between the two states.²⁰⁰ Transition between these two states can occur when external energy is applied, such as pressure²⁰¹, vibration²⁰², electrical field²⁰³. The threshold of the mutual transition is while these two states possess equal apparent CA, i.e. $\theta_W = \theta_{CB}$.²⁰⁴ To combine the Wenzel equation and Cassie equation, the critical apparent CA can be obtained²⁰⁴,

$$\cos\theta_C = (f_{SW} - 1)/(r - f_{SW}) \quad (4)$$

where θ_C is the critical apparent CA to transit between the two states. Because $f_{SW} < 1 < r$, $-1 < \cos\theta_C < 0$, i.e. $\theta_C > 90^\circ$. While $90^\circ < \theta_0 < \theta_C$, the air trapped is unstable, the Cassie state easily

transit to the Wenzel state; while $\theta_0 > \theta_C$, the Cassie state stable. For a certain material, the Young's CA is constant. In order to obtain stable self-cleaning surface, we can adjust the surface geometric structure to minimize the θ_C .

To fabricate an in-air superoleophobic surface is much more difficult than that of superhydrophobic surface because oils commonly smaller surface free energy than water. And this is the fundamental reason that oils can be separated from water. To fabricate a superhydrophobic surface, as illustrated by Wenzel and Cassie equations, increase of surface roughness and decrease of surface free energy is efficient ways. However, to fabricate a superoleophobic surface, researchers commonly construct the re-entrant structure, such as inverted trapezoidal structure, mushroom-like structure and convex structure.²⁰⁵⁻²⁰⁷ The re-entrant structures are more likely to trap air and form stable Cassie wetting state. Theoretical studies revealed that this kind of structure can even form super-lyophobic property on an inherent lyophilic surface.^{206,207}

5.4 Underwater wettability of Oil

While the wetting behaviour is occurred underwater, we first take the CA of an ideally smooth surface into account (Fig. 16d). The wetting equation at solid-water-oil interface can be conducted by combining the Young's equation (eqn(1)) of a solid-air-water interface¹⁹⁶ and a solid-air-oil interface as it was suggested by Jung and Bhushan²⁰⁸. The apparent OCA (θ_{OW}) in an aqueous environment can be given as²⁰⁸

$$\cos\theta_{OW} = \frac{\gamma_{OA}\cos\theta_O - \gamma_{WA}\cos\theta_W}{\gamma_{OW}} \quad (5)$$

where θ_W and θ_O are the WCA and OCA in air. γ_{OA} , γ_{WA} and γ_{OW} are interface tensions of oil-air, water-air and oil-water interfaces respectively. θ_W and θ_O represent the WCA and OCA in air. As predicted by eqn(5), for a hydrophilic surface, the surface is simultaneous oleophilic due to the lower surface tension of oil (γ_{OA}) in air than that of water (γ_{WA}) ($\theta_O < \theta_W < 90^\circ$). Therefore, the values of $\cos\theta_O$ and $\cos\theta_W$ are all positive. Since the surface tensions of oil/organic liquids are much lower than that of water ($\gamma_{OA} < \gamma_{WA}$), the value of $\gamma_{OA}\cos\theta_O - \gamma_{WA}\cos\theta_W$ is commonly negative and thus it can be concluded that most hydrophilic surfaces in air show oleophobic property underwater at the solid-water-oil interfacial. For a hydrophobic ($\theta_W > 90^\circ$) and oleophilic ($\theta_O < 90^\circ$) surface, the surface is always oleophilic in the aqueous media since the value of numerator in the right-hand side of eqn(1) is always larger than 0. For a hydrophobic ($\theta_W > 90^\circ$) and oleophobic ($\theta_O > 90^\circ$) surface, an underwater oleophobic surface can be created if $\gamma_{OA}\cos\theta_O$ is bigger than $\gamma_{WA}\cos\theta_W$. The wettabilities at different interfaces are summarized in Table 2.²⁰⁸

Similar to the Wenzel and Cassie equations in air, the underwater Wenzel equation (Fig. 16e) and Cassie equation (Fig. 16f) can be obtained by introducing the surface roughness and contact phase fractions (solid-oil and solid-water interfaces) Wenzel¹⁹⁷:

$$\cos\theta_W = r\cos\theta_{OW} \quad (6)$$

Cassie¹⁹⁸:

$$\cos\theta_{CB} = r_f f_{SO} \cos\theta_{OW} + f_{SO} - 1 = r_f \cos\theta_{OW} -$$

$$f_{SW}(r_f \cos\theta_{OW} + 1) \quad (7)$$

where f_{SO} is the solid-oil fraction under the contact area. It is obvious that the underwater wettability of oil is also determined by the surface roughness, solid-oil fraction (solid-water fraction), as well as the Young's CA of oil in an aqueous environment.

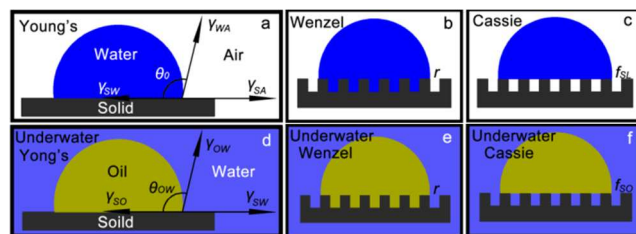


Fig. 16 Sketches showing the in-air and underwater wetting mechanism of water/oil droplets residing on solid surfaces at different wetting states. (a) Water droplet on a smooth surface. Water droplets on rough surfaces with homogenous wetting state (b) and heterogeneous wetting state (c). (d) Underwater oil droplet on a smooth surface. Underwater oil droplets on rough surfaces with homogenous wetting state (e) and heterogeneous wetting state (f).

Table 2 Summary of hydrophilic/hydrophobic natural at various interface²⁰⁸

Solid-air-water interface	Solid-water-oil interface	Solid-water-oil interface
Hydrophilic ($\gamma_{SA} > \gamma_{SW}$)		Oleophobic if $\gamma_{OA}\cos\theta_O < \gamma_{WA}\cos\theta_W$
		Oleophilic if $\gamma_{OA}\cos\theta_O > \gamma_{WA}\cos\theta_W$
Hydrophobic ($\gamma_{SA} < \gamma_{SW}$)	Oleophobic if $\gamma_{SA} < \gamma_{SO}$	Oleophobic if $\gamma_{OA}\cos\theta_O > \gamma_{WA}\cos\theta_W$
	Oleophilic if $\gamma_{SA} > \gamma_{SO}$	Oleophilic if $\gamma_{OA}\cos\theta_O < \gamma_{WA}\cos\theta_W$
		Oleophilic

6. Conclusions

Nowadays, oil leakage and oil-contaminated water need to be addressed urgently since it has become a worldwide issue. Therefore, demands for synthesizing functional materials for efficient treatment of oily water is imperative. In this feature article, we reviewed the development of various special wettability stimulated oil/water separation materials by sorting them into several categories based on the substrate materials they used, from the early superhydrophobic-superoleophilic separation materials (oil-removing materials), to the superhydrophilic and underwater superoleophobic separation materials (water-removing materials), to smart separation materials with switchable wettability. The special wettability stimulated separation materials show big advantages when compared with the conventional oil/water filter materials due to their high selective absorbing/filtering feature. Amazingly, the separation of the oil-in-water emulsions, the water-in-oil emulsions, and even the surfactant-stabilized emulsions were successfully achieved very recently by using the special wettability membranes with a maximum separation efficiency larger than 99.999%. Distinguished from the former separation materials which are usually applied to separate the layered oil-and-water mixture, these membranes possess a smaller and more compact pore size

which can be employed to separate oil-water emulsions with the droplet sizes from the micrometer to the nanometer range. In the last section, the theories involved for both the oil-removing process and water-removing process are discussed from the view of balanced condition of force. Here, particular attention is paid to summarizing and comparing the separation efficiencies, absorption capacities and recyclabilities which are crucial for the practical usage in oil spill accidents to oil/water separation materials.

Although the special wettability stimulated oil/water separation materials show their enormous potential in the treatment of oil spill accident and the industrial oily water, the investigations in this field are still facing a lot of challenges, and some of the problems still need to be solved before they can be used to replace the traditional separation techniques, as well as for the further studies. First and foremost, design and synthesis of stable and durable rough surface structure on materials with special wettability is a big challenge. Original porous substrate materials usually provide the pre-existing micro-scale rough structure, to obtain an extreme wetting state, a layer of nano-scale structure is needed to form the typically hierarchical structure. However, most of the surface fine structures can be easily damaged by the external influences including mechanical stress and chemical contamination, which restricts the material's applications. Secondary, the oil (water) filtering materials (such as fabric- and metallic mesh-based materials) are unrealistic to be directly used for oil leakage treatment for the oily water which should be collected in advance so as to realize the gravity driven oil/water separation. Thirdly, a large portion of the synthesis methods can be hardly large-scaled (such as *in situ* growth method and hydrothermal method) and thus the mass-production techniques of oil/water separation materials for the large-area oil spill are still required. Fourth, while the separations of oil/water emulsion have been realized, the separation speed and the membrane pore sizes are considered to be contradictories. Therefore, how to realize effective and high-throughput separation of a wide range of oil/water emulsion with small droplet sizes from the micrometer to the nanometer range is an important issue. Finally, most of the previous works focused on the separation of low-viscous oil-and-water mixtures, the researches about the separation of high-viscous oil-and-water mixtures are vacant.

As we know, the special wettability stimulated oil/water separation materials are commonly inspired from the natural plants (e.g. lotus leaf) and animals (e.g. fish scale) that exhibit special wettability. To achieve the industrialization of bio-inspired oil/water separation materials at an early date, our future works will mainly concentrate on four aspects as follows: first, by combining theoretical prediction, wear-resistant oil/water separation materials are aimed to be designed and synthesized to increase the materials' life time. Second, more and more simple and large-scaled preparation methods are being searched to achieve industrialization in oil/water separation. Third, efficient and rapidly separation materials of oil/water emulsion with ultra-small droplets should be taken into consideration. Fourth, specialized materials will be developed for the rapid separation of high-viscous oil-and-water mixture. Finally, multifunctional (such as magnetic oil-removing materials) and external stimulate-responsive (from single to dual and even to multiple stimulate-

responsive) materials are also need to be considered to synthesis smart interfacial materials for different oil/water separation purpose.

Acknowledgments

This work is supported by the National Nature Science Foundation of China (NO11172301 and 21203217), the "Funds for Distinguished Young Scientists" of Hubei Province (2012FFA002), the "Western Light Talent Culture" Project, the Co-joint Project of Chinese Academy of Sciences and the "Top Hundred Talents" Program of Chinese Academy of Sciences and the National 973 Project (2013CB632300) for financial support.

Notes and references

- ^a Hubei Collaborative Innovation Centre for Advanced Organic Chemical Materials and Ministry of Education Key Laboratory for the Green Preparation and Application of Functional Materials, Hubei University, Wuhan 430062, People's Republic of China. Fax: 0086-931-8277088; Tel: 0086-931-4968105; E-mail: zguo@licp.cas.cn
- ^b State Key Laboratory of Solid Lubrication, Lanzhou Institute of Chemical Physics, Chinese Academy of Sciences, Lanzhou 730000, People's Republic of China
- † Ben Wang and Weixin Liang contribute equally to this work.
- J. W. Short, S. D. Rice, R. A. Heintz, M. G. Carls and A. Moles, *Energy Sources*, 2003, **25**, 509–517.
 - B. Dubansky, A. Whitehead, J. T. Miller, C. D. Rice and F. Galvez, *Environ. Sci. Technol.*, 2013, **47**, 5074–5082.
 - A. B. Nordvik, J. L. Simmons, K. R. Bitting, A. Lewisa and T. S.-Kristiansen, *Spill Sci. Technol. Bull.*, 1996, **3**, 107–122.
 - K. Gaaseidnes and J. Turbeville, *Pure Appl. Chem.*, 1999, **71**, 95–101.
 - B. Tansel and J. Regula, *J. Environ. Sci. Health. Part A Toxic/Hazard. Subst. Environ. Eng.*, 2000, **35**, 1557–1575.
 - D. Quéré, *Annu. Rev. Mater. Res.*, 2008, **38**, 71–99.
 - D. Bonn, J. Eggers, J. Indekeu, J. Meunier and E. Rolley, *Rev. Mod. Phys.*, 2009, **81**, 739–805.
 - (a) Y. B. Zhang, Y. Chen, L. Shi, J. Li and Z. G. Guo, *J. Mater. Chem.*, 2012, **22**, 799–815. (b) G. Y. Wang, Z. G. Guo and W. M. Liu, *J. Bionic and Engineer.* 2014, **11**, 325–345.
 - M. J. Liu, S. T. Wang and L. Jiang, *MRS Bull.*, 2013, **38**, 375–382.
 - B. Bhushan and Y. C. Jung, *Prog. Mater. Sci.*, 2011, **56**, 1–108.
 - X. J. Feng and L. Jiang, *Adv. Mater.*, 2006, **18**, 3063–3078.
 - N. Gao, Y. Y. Yan, *Nanoscale*, 2012, **4**, 2202–2218.
 - X. Zhang, F. Shi, J. Niu, Y. G. Jiang and Z. Q. Wang, *J. Mater. Chem.*, 2008, **18**, 621–633.
 - Z. X. Xue, M. J. Liu and L. Jiang, *J. Polym. Sci., Part B: Polym. Phys.*, 2012, **50**, 1209–1224.
 - Y. Huang, M. J. Liu, J. X. Wang, J. M. Zhou, L. B. Wang, Y. L. Song and L. Jiang, *Adv. Funct. Mater.*, 2011, **21**, 4436–4441.
 - L. Lin, M. J. Liu, L. Chen, P. P. Chen, J. Ma, D. Han and L. Jiang, *Adv. Mater.*, 2010, **22**, 4826–4830.
 - M. J. Liu, Z. X. Xue, H. Liu and L. Jiang, *Angew. Chem. Int. Ed.*, 2012, **51**, 8348–8351.
 - Z. Burton and B. Bhushan, *Ultramicroscopy*, 2006, **106**, 709–719.
 - A. Poynor, L. Hong, I. K. Robinson, S. Granick, Z. Zhang and P. A. Fenter, *Phys. Rev. Lett.*, 2006, **97**, 266101–266104.
 - T. Onda, S. Shibuichi, N. Satoh and K. Tsujii, *Langmuir*, 1996, **12**, 2125–2127.
 - J. Bico, C. Marzolin and D. Quéré, *Europhys. Lett.*, 1999, **47**, 220–226.
 - W. Chen, A. Y. Fadeev, M. C. Hsieh, D. Öner, J. Youngblood and T. J. McCarthy, *Langmuir*, 1999, **15**, 3395–3399.
 - R. Blossy, *Nat. Mater.*, 2003, **2**, 301–306.
 - L. W. Zhang, R. Dillert, D. Bahnemann and M. Vormoor, *Energy Environ. Sci.*, 2012, **5**, 7491–7507.
 - Y. Chen, Y. B. Zhang, L. Shi, J. Li, Y. Xin, T. T. Yang and Z. G. Guo, *Appl. Phys. Lett.*, 2012, **101**, 033701.

- 26 G. Y. Wang, W. X. Liang, B. Wang, Y. B. Zhang, J. Li, L. Shi and Z. G. Guo, *Appl. Phys. Lett.*, 2013, **102**, 203703.
- 27 S. Nagappan, S. S. Park, E. J. Yu, H. J. Cho, J. J. Park, W.-K. Lee and C.-S. Ha, *J. Mater. Chem. A*, 2013, **1**, 12144-12153.
- 28 M. Elsharkawy, T. M. Schutzius and C. M. Megaridis, *Lab Chip*, 2014, **14**, 1168-1175.
- 29 B. Wang, Y. B. Zhang, W. X. Liang, G. Y. Wang, Z. G. Guo and W. M. Liu, *J. Mater. Chem. A*, 2014, **2**, 7845-7852.
- 30 J. Y. Lv, Y. L. Song, L. Jiang and J. J. Wang, *ACS Nano*, 2014, **8**, 3152-3169.
- 31 H. R. Yang, H. J. Zhu, M. M. R. M. Hendrix, N. J. H. G. M. Lousberg, G. de With, C. C. Esteves and J. H. Xin, *Adv. Mater.*, 2013, **25**, 1150-1154.
- 32 J. Li, L. Shi, Y. Chen, Y. B. Zhang, Z. G. Guo, B. L. Su and W. M. Liu, *J. Mater. Chem.*, 2012, **22**, 9774-9781.
- 33 B. Wang, J. Li, G. Y. Wang, W. X. Liang, Y. B. Zhang, L. Shi, Z. G. Guo and W. M. Liu, *ACS Appl. Mater. Interfaces*, 2013, **5**, 1827-1839.
- 34 W. X. Liang and Z. G. Guo, *RSC Adv.*, 2013, **3**, 16469-16474.
- 35 J. W. Zeng and Z. G. Guo, *Colloids and Surfaces A: Physicochem. Eng. Aspects*, 2014, **444**, 283-288.
- 36 Z. G. Guo, W. M. Liu and B. L. Su, *Appl. Phys. Lett.*, 2008, **92**, 063104.
- 37 Z. G. Guo, F. Zhou, J. C. Hao and W. M. Liu, *J. Am. Chem. Soc.*, 2005, **127**, 15670-15671.
- 38 J. L. Song, S. Huang, K. Hu, Y. Lu, X. Liu and W. Xu, *J. Mater. Chem. A*, 2013, **1**, 14783-14789.
- 39 S. Sethi and A. Dhinojwala, *Langmuir*, 2009, **25**, 4311-4313.
- 40 L. Feng, Z. Y. Zhang, Z. H. Mai, Y. M. Ma, B. Q. Liu, L. Jiang and D. B. Zhu, *Angew. Chem. Int. Ed.*, 2004, **43**, 2012-2014.
- 41 Q. J. Wang, Z. Cui, Y. Xiao and Q. M. Pan, *Appl. Surf. Sci.*, 2010, **256**, 4095-4102.
- 42 H. Li, M. J. Zheng, L. Ma, C. Q. Zhu and S. Lu, *Mater. Res. Bull.*, 2013, **48**, 25-29.
- 43 Y. Z. Cao, X. Y. Zhang, L. Tao, K. Li, Z. X. Xue, L. Feng and Y. Wei, *ACS Appl. Mater. Interfaces*, 2013, **5**, 4438-4442.
- 44 J. An, J.-F. Cui, Z.-Q. Zhu, W.-D. Liang, C.-J. Pei, H.-X. Sun, B.-P. Yang and A. Li, *J. Appl. Polym. Sci.*, 2014, DOI: 10.1002/APP.40759.
- 45 W. X. Liang and Z. G. Guo, *RSC Adv.*, 2013, **3**, 16469-16474.
- 46 B. C. Li, L. X. Li, L. Wu, J. P. Zhang and A. Q. Wang, *ChemPlusChem*, 2014, **79**, 850-856.
- 47 S. T. Wang, Y. L. Song and L. Jiang, *Nanotechnology*, 2007, **18**, 015103.
- 48 B. Wang and Z. G. Guo, *Appl. Phys. Lett.*, 2013, **103**, 063704.
- 49 C. X. Wang, T. J. Yao, J. Wu, C. Ma, Z. X. Fan, Z. Y. Wang, Y. R. Cheng, Q. Lin and B. Yang, *ACS Appl. Mater. Interfaces*, 2009, **11**, 2613-2617.
- 50 C. R. Gao, Z. X. Sun, K. Li, Y. N. Chen, Y. Z. Cao, S. Y. Zhang and L. Feng, *Energy Environ. Sci.*, 2013, **6**, 1147-1151.
- 51 Y. Z. Yang, H. D. Li, S. H. Cheng, G. T. Zou, C. X. Wang and Q. Lin, *Chem. Commun.*, 2014, **50**, 2900-2903.
- 52 C. R. Crick, J. A. Gibbins and I. P. Parkin, *J. Mater. Chem. A*, 2013, **1**, 5943-5948.
- 53 C. Lee and S. Baik, *Carbon*, 2010, **48**, 2192-2197.
- 54 C. H. Lee, N. Johnson, J. Drelich and Y. K. Yap, *Carbon*, 2011, **49**, 669-676.
- 55 D. L. Tian, X. F. Zhang, X. Wang, J. Zhai and L. Jiang, *Phys. Chem. Chem. Phys.*, 2011, **12**, 14606.
- 56 H. Li, Y. S. Li and Q. Z. Liu, *Nanoscale Res. Lett.*, 2013, **8**, 183.
- 57 H. X. Sun, A. Li, X. J. Qin, Z. Q. Zhu, W. D. Liang, J. An, P. Q. La and W. Q. Deng, *ChemSusChem*, 2013, **6**, 2377-2381.
- 58 D. Deng, D. P. Prendergast, J. MacFarlane, R. Bagatin, F. Stellacci and P. M. Gschwend, *ACS Appl. Mater. Interfaces*, 2013, **5**, 774-781.
- 59 F. J. Wang, S. Lei, M. S. Xue, J. F. Ou, C. Q. Li and W. Li, *J. Phys. Chem. C*, 2014, **118**, 6344-6351.
- 60 M. J. Cheng, G. N. Ju, C. Jiang, Y. J. Zhang and F. Shi, *J. Mater. Chem. A*, 2013, **1**, 13411-13416.
- 61 B. Cortese, D. Caschera, G. Padeletti, G. M. Ingo and G. Gigli, *Surface Innovations*, 2013, **1**, 140-156.
- 62 Y. Y. Liu, J. H. Xin and C.-H. Choi, *Langmuir*, 2012, **28**, 17426-17434.
- 63 Q. F. An, W. Xu, L. F. Hao, Y. S. Fu and L. X. Huang, *J. Appl. Polym. Sci.*, 2013, **128**, 3050-3056.
- 64 H. Zhou, H. X. Wang, H. T. Niu, A. Gestos, and T. Lin, *Adv. Funct. Mater.*, 2013, **23**, 1664-1670.
- 65 B. X. Leng, Z. Z. Shao, G. de With, and W. H. Ming, *Langmuir*, 2009, **25**, 2456-2460.
- 66 C. H. Xue, S. T. Jia, H. Z. Chen and M. Wang, *Sci. Technol. Adv. Mater.*, 2008, **9**, 035001.
- 67 M. Zhang, C. Y. Wang, S. L. Wang and J. Li, *Carbohydr. Polym.*, 2013, **97**, 59-64.
- 68 X. Zhang, T. Geng, Y. G. Guo, Z. J. Zhang and P. Y. Zhang, *Chem. Eng. J.*, 2013, **231**, 414-419.
- 69 X. M. Tang, Y. Si, J. L. Ge, B. Ding, L. F. Liu, G. Zheng, W. J. Luo and J. Y. Yu, *Nanoscale*, 2013, **5**, 11657-11664.
- 70 Y. W. Shang, Y. Si, A. Raza, L. P. Yang, X. Mao, B. Ding and J. Y. Yu, *Nanoscale*, 2012, **4**, 7847-7854.
- 71 J. Y. Lin, F. Tian, Y. W. Shang, F. J. Wang, B. Ding, J. Y. Yu and Z. Guo, *Nanoscale*, 2013, **5**, 2745-2755.
- 72 J. P. Zhang and S. Seeger, *Adv. Funct. Mater.*, 2011, **21**, 4699-4704.
- 73 J. F. Wang, T. Tsuzuki, B. Tang, L. Sun, X. J. Dai, G. D. Rajmohan, J. L. Li and X. G. Wang, *Aust. J. Chem.*, 2013, **67**, 71-77.
- 74 J. T. Wang, Y. Zheng and A. Q. Wang, *Chem. Eng. J.*, 2012, **213**, 1-7.
- 75 J. Wu, N. Wang, H. Dong, Y. Zhao, and L. Jiang, *ACS Appl. Mater. Interfaces*, 2012, **4**, 3207-3212.
- 76 J. Zhao, C. F. Xiao and N. K. Xu, *Environ. Sci. Pollut. Res.*, 2013, **20**, 4137-4145.
- 77 B. Deng, R. Cai, Y. Yu, H. Q. Jiang, C. L. Wang, J. Li, L. F. Li, M. Yu, J. Y. Li, L. D. Xie, Q. Huang and C. H. Fan, *Adv. Mater.*, 2010, **22**, 5473-5477.
- 78 J. P. Zhang, B. C. Li, L. Wu and A. Q. Wang, *Chem. Commun.*, 2013, **49**, 11509-11511.
- 79 L. Wu, J. P. Zhang, B. C. Li and A. Q. Wang, *J. Mater. Chem. B.*, 2013, **1**, 4756-4763.
- 80 L. Wu, J. P. Zhang, B. C. Li and A. Q. Wang, *Polym. Chem.*, 2014, **5**, 2382-2390.
- 81 X. Y. Zhou, Z. Z. Zhang, X. H. Xu, F. Guo, X. T. Zhu and X. H. Men, *ACS Appl. Mater. Interfaces*, 2013, **5**, 7208-7214.
- 82 J. Zimmermann, F. A. Reifler, G. Fortunato, L.-C. Gerhardt and S. Seeger, *Adv. Funct. Mater.*, 2008, **18**, 3662-3669.
- 83 J. Li, L. Shi, Y. Chen, Y. B. Zhang, Z. G. Guo, B. L. Su and W. M. Liu, *J. Mater. Chem.*, 2012, **22**, 9774-9781.
- 84 B. Wang, J. Li, G. Y. Wang, W. X. Liang, Y. B. Zhang, L. Shi, Z. G. Guo and W. M. Liu, *ACS Appl. Mater. Interfaces*, 2013, **5**, 1827-1839.
- 85 J. Li, L. Shi, Y. Chen, Y. B. Zhang, Z. G. Guo, B. L. Su and W. M. Liu, *J. Mater. Chem.*, 2012, **22**, 9774-9781.
- 86 D. D. Nguyen, N.-H. Tai, S.-B. Lee and W.-S. Kuo, *Energy Environ. Sci.*, 2012, **5**, 7908-7912.
- 87 A. Li, H. X. Sun, D. Z. Tan, W. J. Fan, S. H. Wen, X. J. Qing, G. X. Li, S. Y. Li and W.-Q. Deng, *Energy Environ. Sci.*, 2011, **4**, 2062-2065.
- 88 Q. Zhu, Q. M. Pan and F. T. Liu, *J. Phys. Chem. C*, 2011, **115**, 17464-17470.
- 89 L. B. Zhang, Z. H. Zhang and P. Wang, *NPG Asia Mater.*, 2012, **4**, e8.
- 90 S.-J. Choi, T.-H. Kwon, H. Im, D.-I. Moon, D. J. Baek, M.-L. Seol, J. P. Duarte and Y.-K. Choi, *ACS Appl. Mater. Interfaces*, 2011, **3**, 4552-4556.
- 91 X. Y. Zhou, Z. Z. Zhang, X. H. Xu, X. H. Men and X. T. Zhu, *Ind. Eng. Chem. Res.*, 2013, **52**, 9411-9416.
- 92 G. H. Jiang, R. B. Hu, X. G. Xi, X. H. Wang and R. J. Wang, *J. Mater. Res.*, 2013, **28**, 651-656.
- 93 X. Y. Zhang, Z. Li, K. S. Liu and L. Jiang, *Adv. Funct. Mater.*, 2013, **22**, 2881-2886.
- 94 Q. Zhu, Y. Chu, Z. K. Wang, N. Chen, L. Lin, F. T. Liu and Q. M. Pan, *J. Mater. Chem. A*, 2013, **1**, 5386-5393.
- 95 H. D. Liu, Z. Y. Liu, M. B. Yang and Q. He, *J. Appl. Polym. Sci.*, 2013, **130**, 3530-3536.
- 96 K. S. Liu, and L. Jiang, *ACS Nano*, 2011, **5**, 6786-6790.

- 97 P. Calcagnile, D. Fragouli, I. S. Bayer, G. C. Anyfantis, L. Martiradonna, P. D. Cozzoli, R. Cingolani and A. Athanassiou, *ACS Nano*, 2012, **6**, 5413-5419.
- 98 Q. Zhu and Q. M. Pan, *ACS Nano*, 2014, **8**, 1402-1409.
- 5 99 C. Wu, X. Y. Huang, X. F. Wu, R. Qian and P. K. Jiang, *Adv. Mater.*, 2013, **25**, 5658-5662.
- 100 H. X. Sun, A. Li, Z. Q. Zhu, W. D. Liang, X. H. Zhao, P. Q. La and W. Q. Deng, *ChemSusChem*, 2013, **6**, 1057-1062.
- 101 E. Singh, Z. Chen, F. Houshmand, W. Ren, Y. Peles, H.-M. Cheng and N. Koratkar, *Small*, 2013, **9**, 75-80.
- 102 X. Dong, J. Chen, Y. Ma, J. Wang, M. B. Chan-Park, X. Liu, L. Wang, W. Huang and P. Chen, *Chem. Commun.*, 2012, **48**, 10660-10662.
- 103 Z. L. Fan, X. J. Qin, H. X. Sun, Z. Q. Zhu, C. J. Pei, W. D. Liang, X. M. Bao, J. An, P. Q. La, A. Li and W. Q. Deng, *ChemPlusChem*, 2013, **78**, 1282-1287.
- 15 104 X. D. Huang, B. Sun, D. W. Su, D. Y. Zhao and G. X. Wang, *J. Mater. Chem. A*, 2014, **2**, 7973-7979.
- 105 Y. Yang, Z. Tong, T. Ngai and C. Y. Wang, *ACS Appl. Mater. Interfaces*, 2014, **6**, 6351-6360.
- 20 106 H. C. Bi, Z. Y. Yin, X. H. Cao, X. Xie, C. L. Tan, X. Huang, B. Chen, F. T. Chen, Q. L. Yang, X. Y. Bu, X. H. Lu, L. T. Sun and H. Zhang, *Adv. Mater.*, 2013, **25**, 5916-5921.
- 107 Z. Y. Wu, C. Li, H. W. Liang, J. F. Chen and S. H. Yu, *Angew. Chem. Int. Ed.*, 2013, **52**, 2925-2929.
- 25 108 H. W. Liang, Q. F. Guan, L. F. Chen, Z. Zhu, W. J. Zhang and S. H. Yu, *Angew. Chem. Int. Ed.*, 2012, **51**, 5101-5105.
- 109 H. Y. Sun, Z. Xu and C. Gao, *Adv. Mater.*, 2013, **25**, 2554-2560.
- 110 H. C. Bi, X. Xie, K. B. Yin, Y. L. Zhou, S. Wan, L. B. He, F. Xu, F. Banhart, L. T. Sun and R. S. Ruoff, *Adv. Funct. Mater.*, 2012, **22**, 4421-4425.
- 30 111 Y. Q. He, Y. Liu, T. Wu, J. K. Ma, X. R. Wang, Q. J. Gong, W. N. Kong, F. B. Xing, Y. Liu and J. P. Gao, *J. Hazard. Mater.*, 2013, **260**, 796-805.
- 112 Y. Zhao, C. G. Hu, Y. Hu, H. H. Cheng, G. Q. Shi and L. T. Qu, *Angew. Chem. Int. Ed.*, 2012, **51**, 11371-11375.
- 35 113 C. B. Chen, R. Li, L. M. Xu and D. Y. Yan, *RSC Adv.*, 2014, **4**, 17393-17400.
- 114 H.-P. Cong, X.-C. Ren, P. Wang and S.-H. Yu, *ACS Nano*, 2012, **6**, 2693-2703.
- 40 115 X. C. Gui, J. Q. Wei, K. L. Wang, A. Y. Cao, H. W. Zhu, Y. Jia, Q. K. Shu and D. H. Wu, *Adv. Mater.*, 2010, **22**, 617-621.
- 116 X. H. Gui, H. B. Li, K. L. Wang, J. Q. Wei, Y. Jia, Z. Li, L. L. Fan, A. Y. Cao, H. W. Zhu and D. H. Wu, *Acta Mater.*, 2011, **59**, 4798-4804.
- 45 117 K. Zhu, Y. Y. Shang, P. Z. Sun, Z. Li, X. M. Li, J. Q. Wei, K. L. Wang, D. H. Wu, A. Y. Cao and H. W. Zhu, *Front. Mater. Sci.*, 2013, **7**, 170-176.
- 118 W. Dai, S. J. Kim, W.-K. Seong, S. H. Kim, K.-R. Lee, H.-Y. Kim and M.-W. Moon, *Sci. Rep.*, 2013, **3**, 2524.
- 50 119 N. Chen and Q. M. Pan, *ACS Nano*, 2013, **7**, 6875-6883
- 120 Y. Chu and Q. M. Pan, *ACS Appl. Mater. Interfaces*, 2012, **4**, 2420-2425.
- 121 X. C. Gui, Z. P. Zeng, Z. Q. Lin, Q. M. Gan, R. Xiang, Y. Zhu, A. Y. Cao and Z. K. Tang, *ACS Appl. Mater. Interfaces*, 2013, **5**, 5845-5850.
- 55 122 T. Arbatan, X. Y. Fang and W. Shen, *Chem. Eng. J.*, 2011, **166**, 787-791.
- 123 B. Akhavan, K. Jarvis and P. Majewski, *ACS Appl. Mater. Interfaces*, 2013, **5**, 8563-8571.
- 60 124 S. J. Liu, Y. J. Li, Y. M. Wang, X. Liu and E. S. Yeung, *J. Colloid Interface Sci.*, 2013, **407**, 243-249.
- 125 X. S. Wang, J. Liu, J. M. Bonefont, D. Q. Yuan, P. K. Thallapally and S. Q. Ma, *Chem. Commun.*, 2013, **49**, 1533-1535.
- 126 X. H. Li, Y. C. Guo, J. Zhang and L. Zhang, *J. Appl. Polym. Sci.*, 2013, **128**, 2994-2999.
- 65 127 F. Novio and D. Ruiz-Molina, *RSC Adv.*, 2014, **4**, 15293-15296.
- 128 W. W. Lei, D. Portehault, D. Liu, S. Qin and Y. Chen, *Nat. Commun.*, 2013, **4**, 1777.
- 129 A. Sarkar and S. Mahapatra, *J. Mater. Chem., A*, 2014, **2**, 3808-3818.
- 70 130 K. Dutta and A. Pramanik, *Chem. Commun.*, 2013, **49**, 6427-6429.
- 131 L. P. Xu, X. W. Wu, J. X. Meng, J. T. Peng, Y. Q. Wen, X. J. Zhang and S. T. Wang, *Chem. Commun.*, 2013, **49**, 8752-8754
- 132 A. Banerjee, R. Gokhale, S. Bhatnagar, J. Jog, M. Bhardwaj, B. Lefez, B. Hannoyer and S. Ogale, *J. Mater. Chem.*, 2012, **22**, 19694-19699.
- 75 133 W. X. Liang, G. Y. Wang, B. Wang, Y. B. Zhang and Z. G. Guo, *Acta Chim. Sinica*, 2013, **71**, 639-643.
- 134 Q. Zhu, F. Tao and Q. M. Pan, *ACS Appl. Mater. Interfaces*, 2010, **2**, 3141-3146.
- 80 135 L. Zhang, J. J. Wu, Y. X. Wang, Y. H. Long, N. Zhao and J. Xu, *J. Am. Chem. Soc.*, 2012, **134**, 9879-9881.
- 136 P. Tempesti, M. Bonini, F. Ridi and P. Baglioni, *J. Mater. Chem. A*, 2014, **2**, 1980-1984.
- 137 S. W. Zhang, M. Y. Zeng, J. X. Li, J. Li, J. Z. Xu and X. K. Wang, *J. Mater. Chem. A*, 2014, **2**, 4391-4397.
- 85 138 Z. Zhang, G. Sèbe, D. Rentsch, T. Zimmermann and P. Tingaut, *Chem. Mater.*, 2014, **26**, 2659-2668.
- 139 X. T. Zhu, Z. Z. Zhang, G. N. Ren, J. Yang, K. Wang, X. H. Xu, X. H. Men and X. Y. Zhou, *J. Mater. Chem.*, 2012, **22**, 20146-20148.
- 90 140 B. Ge, Z. Z. Zhang, X. T. Zhu, G. N. Ren, X. H. Men and X. Y. Zhou, *Colloids and Surface A: Physicochem. Eng. Aspect*, 2013, **429**, 129-133.
- 141 G. Hayase, K. Kanamori, M. Fukuchi, H. Kaji and K. Nakanishi, *Angew. Chem. Int. Ed.*, 2013, **52**, 1986-1989.
- 95 142 S. H. Wang, M. Li and Q. H. Lu, *ACS Appl. Mater. Interfaces*, 2010, **2**, 677-683.
- 143 M. Zhang, C. Y. Wang, S. L. Wang, Y. L. Shi and J. Li, *Appl. Surf. Sci.*, 2012, **261**, 764-769.
- 144 Z. X. Xue, Z. X. Sun, Y. Z. Cao, Y. N. Chen, L. Tao, K. Li, L. Feng, Q. Fu and Y. Wei, *RSC Adv.*, 2013, **3**, 23432-23437.
- 100 145 M. J. Cheng, Y. F. Gao, X. P. Guo, Z. Y. Shi, J.-F. Chen, F. Shi, *Langmuir*, 2011, **27**, 7371-7375.
- 146 M. J. Cheng, G. N. Ju, C. Jiang, Y. J. Zhang and F. Shi, *J. Mater. Chem. A*, 2013, **1**, 13411-13416.
- 105 147 J. Ge, Y. D. Ye, H. B. Yao, X. Zhu, X. Wang, L. Wu, J. L. Wang, H. Ding, N. Yong, L. H. He and S. H. Yu, *Angew. Chem. Int. Ed.*, 2014, **53**, 3612-3616.
- 148 M. J. Liu, S. T. Wang, Z. X. Wei, Y. L. Song and L. Jiang, *Adv. Mater.*, 2009, **21**, 665-669.
- 110 149 L.-P. Xu, J. Zhao, B. Su, X. L. Liu, J. T. Peng, Y. B. Liu, H. L. Liu, G. Yang, L. Jiang, Y. Q. Wen, X. J. Zhang and S. T. Wang, *Adv. Mater.*, 2013, **25**, 606-611.
- 150 M. Nosonovsky and B. Bhushan, *Phil. Trans. R. Soc. A*, 2009, **367**, 1511-1539.
- 115 151 B. Wang, Z. G. Guo and W. M. Liu, *RSC Adv.*, 2014, **4**, 14684-14690.
- 152 A. Raza, B. Ding, G. Zainab, M. El-Newehy, S. S. Al-Deyab and J. Y. Yu, *J. Mater. Chem. A*, 2014, **2**, 10137-10145.
- 153 L. B. Zhang, Y. J. Zhong, D. Cha and P. Wang, *Sci. Rep.*, 2013, **3**, 2326.
- 120 154 Z. X. Xue, S. T. Wang, L. Lin, L. Chen, M. J. Liu, L. Feng and L. Jiang, *Adv. Mater.*, 2011, **23**, 4270-4273.
- 155 Y. Dong, J. Li, L. Shi, X. B. Wang, Z. G. Guo and W. M. Liu, *Chem. Commun.*, 2014, **50**, 5586-5589.
- 125 156 Q. Wen, J. C. Di, L. Jiang, J. H. Yu and R. R. Xu, *Chem. Sci.*, 2013, **4**, 591-595.
- 157 F. Zhang, W. B. Zhang, Z. Shi, D. Wang, J. Jin and L. Jiang, *Adv. Mater.*, 2013, **25**, 4192-4198.
- 158 N. Liu, Y. N. Chen, F. Lu, Y. Z. Cao, Z. X. Xue, K. Li, L. Feng, and Y. Wei, *ChemPhysChem*, 2013, **14**, 3489-3494.
- 130 159 K. Liao, X. Y. Ye, P. C. Chen, Z. K. Xu, *J. Appl. Polym. Sci.*, 2013, DOI: 10.1002/APP.39897.
- 160 J. Drelich and E. Chibowski, *Langmuir*, 2010, **26**, 18621-18623.
- 161 S. Song, L. Q. Jing, S. D. Li, H. G. Fu and Y. B. Luan, *Mater. Lett.*, 2008, **62**, 3503-3505.
- 135 162 T. Darmanin and F. Guittard, *J. Mater. Chem.*, 2009, **19**, 7130.
- 163 A. Steele, I. Bayer and E. Loth, *Nano Lett.*, 2009, **9**, 501-505.
- 164 B. X. Leng, Z. Z. Shao, G. D. With and W. H. Ming, *Langmuir*, 2009, **25**, 2456-2460.
- 140 165 S. J. Hutton, J. M. Crowther and J. P. S. Badyal, *Chem. Mater.*, 2000, **12**, 2282-2286.

- 166 J. A. Howarter and J. P. Youghblood, *Adv. Mater.*, 2009, **19**, 3838-3843.
- 167 J. A. Howarter, K. L. Genson and J. P. Youghblood, *ACS Appl. Mater. Interfaces*, 2011, **3**, 2022-2030.
- 5 168 J. Yang, Z. Z. Zhang, X. H. Xu, X. T. Zhu, X. H. Men and X. Y. Zhou, *J. Mater. Chem.*, 2012, **22**, 2834-2837.
- 169 A. K. Kota, G. Kwon, W. Choi, J. M. Mabry and A. Tuteja, *Nat. Commun.*, 2012, **3**, 1025.
- 170 B. W. Xi and J. C. Hao, *Chem. Soc. Rev.*, 2010, **39**, 769-782.
- 10 171 F. Xia, Y. Zhu, L. Feng and L. Jiang, *Soft Matter*, 2009, **5**, 275-281.
- 172 X. J. Feng, L. Feng, M. H. Jin, J. Zhai, L. Jiang and D. B. Zhu, *J. Am. Chem. Soc.*, 2004, **126**, 62-63.
- 173 T. L. Sun, G. J. Wang, L. Feng, B. Q. Liu, Y. M. Ma, L. Jiang and D. B. Zhu, *Angew. Chem. Int. Ed.*, 2004, **43**, 357-360.
- 15 174 L. Xu, W. Chen, A. Mulchandani and Y. Yan, *Angew. Chem. Int. Ed.*, 2005, **44**, 6009-6012.
- 175 X. Yu, Z. Q. Wang, Y. G. Jiang, F. Shi and X. Zhang, *Adv. Mater.*, 2005, **17**, 1289-1293.
- 176 M. J. Cheng, Q. Liu, G. N. Ju, Y. J. Zhang, L. Jiang and F. Shi, *Adv. Mater.*, **26**, 306-310.
- 20 177 B. Wang and Z. G. Guo, *Chem. Commun.*, 2013, **49**, 9416-9418.
- 178 D. L. Tian, X. F. Zhang, Y. Tian, Y. Wu, X. Wang, J. Zhai and L. Jiang, *J. Mater. Chem.*, 2012, **22**, 19652-19657.
- 179 A. J. Khopade and F. Caruso, *Langmuir*, 2002, **18**, 7669-7676.
- 25 180 H. S. Lim, J. T. Han, D. Kwak, M. Jin and K. Cho, *J. Am. Chem. Soc.*, 2006, **128**, 14458-14459.
- 181 B. L. Xue, L. C. Gao, Y. P. Hou, Z. W. Liu and L. Jiang, *Adv. Mater.*, 2013, **25**, 273-277.
- 182 G. Kwon, A. K. Kota, Y. X. Li, A. Sohani, J. M. Mabry and A. Tuteja, *Adv. Mater.*, 2012, **24**, 3666-3671.
- 30 183 C. McAuliffe, *J. Phys. Chem.*, 1966, **70**, 1267-1275.
- 184 W. B. Zhang, Z. Shi, F. Zhang, X. Liu, J. Jin and L. Jiang, *Adv. Mater.*, 2013, **25**, 2071-2076.
- 185 Z. Shi, W. B. Zhang, F. Zhang, X. Liu, D. Wang, J. Jin and L. Jiang, *Adv. Mater.*, 2013, **25**, 2422-2427.
- 35 186 Y. C. Wang, S. Y. Tao and Y. L. An, *J. Mater. Chem. A*, 2013, **1**, 1701-1708.
- 187 C.-F. Wang and S.-J. Lin, *ACS Appl. Mater. Interfaces*, 2013, **5**, 8861-8864.
- 40 188 Y. Z. Zhu, F. Zhang, D. Wang, X. F. Pei, W. B. Zhang and J. Jin, *J. Mater. Chem. A*, 2013, **1**, 5758-5765.
- 189 W. B. Zhang, Y. Z. Zhu, X. Liu, D. Wang, J. Y. Li, L. Jiang and J. Jin, *Angew. Chem. Int. Ed.*, 2014, **53**, 856-860.
- 190 H. C. Yang, K. J. Liao, H. Huang, Q. Y. Wu, L. S. Wan and Z. K. Xu, *J. Mater. Chem. A*, 2014, **2**, 10225-10230.
- 45 191 X. Wang, X. Chen, K. Yoon, D. Fang, B. S. Hsiao and B. Chu, *Enviro. Sci. Technol.*, 2005, **39**, 7684-7691.
- 192 H. Li, Y. Cao, J. Xin, X. Jie, T. Wang, J. Liu and Q. Yuan, *J. Membr. Sci.*, 2006, **279**, 328-335.
- 50 193 B. Chakrabarty, A. K. Ghoshal and M. K. Purkait, *J. Membr. Sci.*, 2008, **325**, 427-437.
- 194 M. T. M. Pendergast and E. M. V. Hoek, *Energy Environ. Sci.*, 2011, **4**, 1946-1971.
- 195 D. Rana and T. Matsuura, *Chem. Rev.*, 2010, **110**, 2448-2471.
- 55 196 T. Young, *Philos. Trans. R. Soc. London*, 1805, **95**, 65-87.
- 197 R. N. Wenzel, *Ind. Eng. Chem.*, 1936, **28**, 988-994.
- 198 A. Cassie and S. Baxter, *Trans. Faraday Soc.*, 1994, **40**, 546-561.
- 199 Z. L. Chu and S. Seeger, *Chem. Soc. Rev.*, 2014, **43**, 2784-2798.
- 200 M. Nosonovsky and B. Bhushan, *Langmuir*, 2008, **24**, 1525-1533.
- 60 201 P. Forsberg, F. Nikolajeff and M. Karlsson, *Soft Matter*, 2011, **7**, 104-109.
- 202 E. Bormashenko, R. Pogreb, G. Whyman and M. Erlich, *Langmuir*, 2007, **23**, 6501-6503.
- 203 V. Bahadur and S. V. Garimella, *Langmuir*, 2007, **23**, 4918-4924.
- 65 204 A. Lafuma and D. Quéré, *Nat. Mater.*, 2003, **2**, 457-460.
- 205 A. Tuteja, W. Choi, M. Ma, J. M. Mabry, S. A. Mazzella, G. C. Rutledge, G. H. McKinley and R. E. Cohen, *Science*, 2007, **318**, 1618-1622.
- 206 A. Marmur, *Langmuir*, 2008, **24**, 7573-7579.
- 70 207 G. Whyman and E. Bormashenko, *Langmuir*, 2011, **27**, 8171-8176. 208 Y. C. Jung and B. Bhushan, *Langmuir*, 2009, **25**, 14165-14173.

Page 23 of 25		Chemical Society Reviews					
Materials	Preparation methods	WCA (in air)	OCA (in air)	OCA (in water)	Separation or absorption substances	Separation efficiency (%)	Absorption Capacity (Time)
Dimethacrylate-coated nonwoven material	Melt blown spinning method	≥ 127°	0°	n.a.	Crude oil, diesel, toluene	n.a.	7~10
Carbon fabric	<i>In situ</i> vapor phase deposition	156°	0°	n.a.	Hexadecane	97.8	n.a.
Polysulfone membranes	Electrospun and <i>in situ</i> polymerization	161°	0°	n.a.	Dichloromethane	n.a.	n.a.
Electrospun fibrous mats	Co-axial electrospinning	hydrophobic	oleophobic	n.a.	Motor oil, sunflower seed oil	n.a.	47.48~60
Carbon nanotubes coated textiles	Layer-by-layer technique	136°	0°	n.a.	Oil, dodecane, decane, octane	n.a.	up to 2
Cellulose kapok fibers	Sol-gel method	151°	0°	n.a.	n-Hexane, toluene, chloroform, gasoline, diesel, soybean oil	n.a.	41.8~50
Carbon fibers	Electrospinning method	151.3°	0°	n.a.	Diesel oil, silicon oil, peanut oil, motor oil	n.a.	7.13~13
Carbon fabric/ filter paper	One-step dipping process	154° (fabric), 156° (filter paper)	0°	n.a.	Petroleum ether	> 93 for fabric, > 91 for filter paper	n.a.
Ag-coated sponge	<i>In situ</i> growth method	> 150°	0°	n.a.	Hexane, hexadecane, edible oil, chloroform	n.a.	18~30
Triethoxysilane-coated sponges	Vapor-phase deposition process	153.7°	0°	n.a.	Motor oil, lubricating oil, pump oil, silicone oil, soybean oil	n.a.	> 20
Carbon sponges	Dip coating method	162°	0°	n.a.	Motor oil, soybean oil, pump oil, used pump oil, methanol, ethanol, acetone, hexane, chloroform	n.a.	54~160
Carbon coated sponges	Solution-immersion processes	171°	0°	n.a.	Lubricating oil, octane, decane, dodecane	n.a.	> 13
PU sponge	Chromic acid etching	155°	0°	n.a.	Gasoline, crude oil, hexane, petroleum ether	> 95	n.a.
Modified PU sponge	Chemical etching method	157°	0°	n.a.	Decane, dodecane, octane, crude oil, gasoline, bean oil, lubricating oil	Good	15~20
Carbon sponges	Dip-coating method	150.2°	0°	n.a.	Decane, octane, phenixin, benzene, chloroform, kerosene, dichlorobenzene, nitrobenzene, ethanol, acetone, tetrahydrofuran (THF), n-hexane	Good	27.0~80
Carbon fibers coated sponge	Dip-coating after homocoupling polymerization	167°	0°	n.a.	Vegetable oil, pump oil, dodecane, decane, octane, hexane, phenol, nitrobenzene, chloroform, 1,2-dichlorobenzene, ethylbenzene, toluene, benzene, dimethylsulfoxide (DMSO), THF, dimethylformamide (DMF), acetone, ethanol, methanol	Good	6~23
Hydroxyl-oxide modified PU	Amidation procedure followed with grafting	159.1°	Superoleophobic	n.a.	Toluene, gasoline, diesel oil	93.8	26~40
Hydroxyl-oxide modified SiO ₂ /PTFE coated	Chemical vapor deposition after dip coating procedure	165°	0°	n.a.	n-Hexane, pentane, heptane, benzene, toluene, silicone oil	n. a.	10~15
Carbon iron oxide and PU coated foams	Electrostatic deposition technique	160°	0°	n.a.	Mineral oil	n. a.	> 12
Carbon sheets	Dynamic templating approach	165°	0°	n.a.	Ethanol, toluene, pump oil, used engine oil, ethylene glycol	n. a.	20~30
Carbon fish	Mussel-inspired chemistry and Michael addition reaction.	144°	0°	n.a.	Petroleum ether, hexane, gasoline, diesel.	98.12~99.95	n.a.
Carbon mesh	Chemical vapor deposition	157° ± 1°	0°	n.a.	Gasoline, petroleum ether, hexane, diesel	92~97.5	n.a.
Carbon fish	Thermal chemical vapor deposition	163° ± 4°	0°	n.a.	Emulsion (diesel, lubricating oil)	High(need five iterations)	n.a.

Gold mesh	Aerosol assisted chemical vapor deposition	152°~167°	0°	n.a.	Toluene, hexane	> 99	n.a.
Polymers	Electroless metal deposition	Superhydrophobic	0°	n.a.	Dichloromethane, bromobenzene, carbon disulfide, mixed oil	> 90	n.a.
Polymer	Dip-coating	157° ± 2°	4°	n.a.	Diesel oil	> 96	n.a.
Hydrogel	Sol-gel process	152.6°	0°	n.a.	Toluene, TMB, n-hexane, cyclohexane, kerosene, chloroform, petroleum ether, n-octanol, diethylether, n-octane, tetradecane, mineral oil	n.a.	60-150
Hydrogels	Thermal decomposition	162.9° ± 2°	0°	n.a.	N100 Lubricating oil	n.a.	3.7
Polymer powder	Sol-gel process	152°	42° for diesel oil, 25° for crude oil	n.a.	Diesel oil, crude oil	98.1~99.6	n.a.
Gold mesh	Photoinitiated polymerization process	0°	n.a.	155.3°±1.8°	Gasoline, diesel, crude oil, vegetable oil, hexane, petroleum ether.	> 99	n.a.
Hydrogel	Hydrothermal method	0°	n.a.	>150°	Petroleum ether, cyclohexane, soybean oil, diesel, crude oil.	high	n.a.
Gold mesh	Solution-immersion	0°	n.a.	155°	Isooctane, diesel, hexane, petroleum ether, soybean oil.	high	n.a.
Membrane	Dip-coating	0°	152°	n.a.	Oil-in-water emulsion and water-in-oil emulsion	> 99.9	n.a.
Membrane	Vacuum-filtering	94°	0°	n.a.	Water-in-oil emulsions (including surfactant-free and surfactant-stabilized emulsions)	> 99.95	n.a.
Hydrogel sponge	Dip-coating method	162° ± 2°	0°	n.a.	Soybean oil, used motor oil, diesel oil, n-hexadecane, gasoline, n-hexane, water-in-oil emulsions	> 99.97 for water-in-oil emulsion	15-25; Up to 3500 from conjunction with a vacuum system
Hydrogel	Modified-phase inversion process	158°	< 1°	n.a.	Water-in-oil emulsions (including surfactant-free and surfactant-stabilized emulsions)	> 99.95	n.a.
PVDF membrane	SI-ATRP	0°	n.a.	158°	Dispersed oil (including isooctane, hexane, diesel, petroleum ether, soybean oil)	99.999	n.a.
Hydrogels	Pyrolysis method	113.50° ~ 128.64°	0°	n.a.	Methanol, ethanol, ethylene glycol, acetone, n-hexane, 1-octane, cyclohexane, chloroform, phenoxin, acetic ether, ethyl acetoacetate, oleic acid, acetaldehyde, ether, petroleum, THF, ethanediamine, toluene, bromobenzene, styrene, cyclohexene, 1-octadecene, soybean oil, diesel oil, sesame oil, gasoline oil, pump oil.	n.a.	106~312
Hydrogel fiber hydrogels and aerogels (m ⁻³)	Template-directed hydrothermal carbonization process	158° ± 3°	0°	n.a.	Gasoline, cyclohexane, ethanol, diesel oil, vegetable oil, chlorobenzene, phenoxin	n.a.	Up to 115
Hydrogel	Pyrolysis method	hydrophobic	0°	n.a.	Colza oil, olive oil, pump oil, chloroform, toluene, octadecylene, isopropyl alcohol, heptane, hexane, benzylalcohol, DMF, acetone, ethanol, cyclohexane	n.a.	50~190
Hydrogel	Hydrothermal treatment and freeze-drying Hummers method	114° ± 2°	0°	n.a.	Methanol, ethanol, acetone, THF, DMSO, toluene, ethylbenzene, 1,2-dichlorobenzene, chloroform, nitrobenzene, hexane, heptane, octane, dodecane, pump oil, kerosene, castor oil, soybean oil.	n.a.	20~86
Ni/C foams	Template method	152°	0°	n.a.	Bean oil, lubricating oil, crude oil, gasoline, diesel oil, hexane, octane, decane, dodecane	n.a.	Up to 100
Hydrogel	Template method	> 150°	0°	n.a.	Phenixin, NMP, DMSO, nitrobenzene, dodecane, dichlorobenzene, decane, benzene, octane, chloroform, toluene, DMF.	n.a.	7.96-66
Hydrogel	Self-assemble method	> 150°	< 30°	n.a.	Cyclohexane, toluene, gasoline, paraffin oil, vegetable oil, phenoxin.	n.a.	Up to 27

s (m^{-3})	Chemical vapor deposition	156°	0°	n.a.	Hexane, ethanol, gasoline, pump oil, DMF, ethylene glycol, chloroform, mineral oil, vegetable oil, diesel oil, octane, ethyl acetate.	n.a.	80-18
onges (m^{-3})	Chemical vapor deposition	145°	< 4°	n.a.	Diesel oil, gasoline.	n.a.	Up to
ocomposites	Template method	157.2°	0°	n.a.	Lubricating oil, bean oil, crude oil, dodecane, decane.	n.a.	4.5-7.
id foam	Two-step chemical vapor deposition	152.3°	0°	n.a.	Compressor oil, sesame oil, chloroform, dichlorobenzene, toluene, DMF	n.a.	About 80
el (m^{-3})	“Sol-cryo” method	132.9°	0°	n.a.	<i>n</i> -Hexane, ethanol, crude oil, toluene, motor oil, vegetable oil, 1,4-dioxane, ionic liquid, chloroform, phenixin.	n.a.	About 220

Table 1 Summary and comparisons of typical examples for various kinds of oil/water separation materials.